eLife

Reviewed Preprint
v2 • April 16, 2025
Revised by authors

Reviewed Preprint
v1 • June 21, 2024

Computational and Systems Biology

Balancing reaction-diffusion network for cell polarization pattern with stability and asymmetry

Yixuan Chen, Guoye Guan, Lei-Han Tang, Chao Tang

South Bay Interdisciplinary Science Center, Songshan Lake Materials Laboratory, Guangdong, China • Department of Physics, Sichuan University, Sichuan, China • School of Physics, Peking University, Beijing, China • Center for Quantitative Biology, Peking University, Beijing, China • Department of Physics, Hong Kong Baptist University, Hong Kong, China • Institute of Computational and Theoretical Studies, Hong Kong Baptist University, Hong Kong, China • State Key Laboratory of Environmental and Biological Analysis, Hong Kong Baptist University, Hong Kong, China • Peking-Tsinghua Center for Life Sciences, Peking University, Beijing, China

eLife Assessment

This manuscript makes **important** contributions to our understanding of cell polarization dynamics by demonstrating how compensatory regulatory and spatial mechanisms enhance the robustness of polarization patterns. By integrating a computational pipeline with comparisons to experimental data, the authors provide **convincing** evidence that stability and asymmetry in reaction-diffusion networks are crucial for polarization in C. elegans zygotes. Their findings offer novel insights into essential biological processes such as cell migration, division, and symmetry breaking. Future theoretical and experimental work could refine the model by addressing its acknowledged limitations.

https://doi.org/10.7554/eLife.96421.2.sa2

Abstract

Cell polarization is a critical process that separates molecular species into two distinct regions in prokaryotic and eukaryotic cells, guiding biological processes such as cell division and cell differentiation. Although several underlying antagonistic reaction-diffusion networks capable of setting up cell polarization have been identified experimentally and theoretically, our understanding of how to manipulate pattern stability and asymmetry remains incomplete, especially when only a subset of network components are known. Here we present numerical results to show that the polarized pattern of an antagonistic 2-node network collapses into a homogeneous state when subjected to single-sided self-regulation, single-sided additional regulation, or unequal system parameters. However, polarity restoration can be achieved by combining two modifications with opposing effects. Additionally, spatially inhomogeneous parameters favoring respective domains stabilize their interface at designated locations. To connect our findings to cell polarity studies of the nematode *Caenorhabditis elegans* zygote, we reconstituted a 5-node network where a 4-node circuit with full mutual inhibitions between anterior and posterior is modified by a mutual

activation in the anterior and an additional mutual inhibition between the anterior and the posterior. Once again, a generic set of kinetic parameters moves the interface towards either the anterior or posterior end, yet a polarized pattern can be stabilized through spatial tuning of one or more parameters coupled to intracellular or extracellular cues. A user-friendly software, *PolarSim*, is introduced to facilitate the exploration of networks with alternative node numbers, parameter values, and regulatory pathways.

1. Introduction

Cell polarization is a biophysical and biochemical process where a cell acquires spatial anisotropy by establishing directional gradients of molecular species across its membrane or in the cytosol [Knoblich et al., *Nat. Rev. Mol. Cell Biol.*, 2001; Goodrich et al., *Development*, 2011]. Polarity establishment is an essential step in a wide range of biological phenomena, including embryonic development, wound healing, immune activity, and so forth [Etienne-Manneville et al., *Nature*, 2002; Bilder et al. *Science*, 2000]. During cytokinesis, a polarized cell can allocate its molecular contents unequally to its daughter cells, leading to asymmetric cell size and cell fate [Macara, *Nat. Rev. Mol. Cell. Biol.*, 2004]. At the multicellular level, a group of polarized cells can undergo collective movements and constitute stereotypic architectures [Etienne-Manneville et al., *Nature*, 2002; Bilder et al. *Science*, 2000]. Thus, loss or disorder of cell polarization could severely violate normal biological processes, for example, resulting in embryonic lethality and cancerous tumor [Bilder et al., *Science*, 2000; Kim et al., *J. Cell. Sci.*, 2007]. To this day, cell polarization has been a long-term research focus in cell and developmental biology, where more and more efforts have been paid to uncover both the regulatory pathways and design principles involved [Doe et al., *Curr. Opin. Cell Biol.*, 2001; Koorman, *Nat. Cell Biol.*, 2016; Tostevin et al., *Biophys J*, 2008; Chau et al., *Cell*, 2012].

Much of our knowledge on cell polarization is derived from the zygote of the nematode *Caenorhabditis elegans* (referred to as *C. elegans*), which has served as a prominent model organism for studying cell polarization [Rose et al., *WormBook*, 2014; Lang et al., *Development*, 2017]. After fertilization, the *C. elegans* zygote is polarized where the entry side of the sperm (one pole of the ellipsoidal egg) turns into the posterior of the embryo [Goldstein et al., *Development*, 1996; Motegi et al., *Nat. Cell Biol.*, 2011]. Driven by cell polarization, the embryo proceeds tough four successive rounds of asymmetric cell divisions and produces four somatic founder cells sequentially [Sulston et al., *Dev. Biol.*, 1983; Hubatsch et al., *Nat. Phys.*, 2019].

The asymmetric division in the *C. elegans* zygote is governed by a protein family termed partitioning-defective protein (PAR) [Kemphues et al., *Cell*, 1988]. The initial PAR family only consisted of the PAR-3/PAR-6/PKC-3 complex and PAR-1/PAR-2 complex, which are stably accumulated in the anterior and posterior domains on the membrane of the zygote before its division, respectively [Cuenca et al., *Development*, 2003]. During the establishment phase triggered by the sperm entry that defines the zygote's posterior, PAR-3/PAR-6/PKC-3, initially distributed across the entire cell membrane, are anteriorly directed and localized through the contraction of the cortical actomyosin marked by non-muscle myosin II (NMY-2), which allows the PAR-2 (along with the recruitment of PAR-1) to be enriched on the posterior membrane conversely [Rose et al., *WormBook*, 2014; Lang et al., *Development*, 2017]. Subsequently, the maintenance phase follows as the cortical actomyosin contracts halfway across the zygote, with cortical NMY-2 being regulated downstream by PAR proteins and playing a minor role in maintaining the cell polarization pattern [Goehring et al., *J. Cell Biol.*, 2011; Rose et al., *WormBook*, 2014; Beatty et al., *Development*, 2013]. The cell polarization patterns, defined by the concentration distributions of PAR proteins, are stably maintained to guide the assembly of the cytokinetic ring, which is vital for the first asymmetric cell division [Goehring et al., *J. Cell Biol.*, 2011; Rose et al., *WormBook*, 2014; Jankele et al., *eLife*, 2021].

A series of experiments (including RNA interference, immunoprecipitations, fluorescence recovery after photobleaching, and time-lapse single-molecule imaging) further uncovered the mutual inhibition between PAR-3/PAR-6/PKC-3 and PAR-1/PAR-2 upon their association with the membrane and demonstrated its essential role in their robust spatial separation [Cuenca et al., *Development*, 2003; Motegi et al., *Nat. Cell Biol.*, 2011]. Soon, theoretical and numerical studies proved that mutual inhibition forms the backbone (hereafter referred to as an antagonistic 2-node network) of a polarized pattern [Tostevin et al., *Biophys J*, 2008; Chau et al., *Cell*, 2012]. In the *C. elegans* zygote, the antagonism between these two protein groups directs the uneven distribution in downstream cell fate determinants (*e.g.*, PIE-1 and P granules), which is inherited by the two daughter cells during the following asymmetric cell division, leading to cell differentiation [Schubert et al., *Mol. Cell*, 2000; Wang et al., *Adv. Exp. Med. Biol.*, 2013].

In recent years, more proteins have been identified to significantly interact with the antagonistic 2-node network during the maintenance phase of *C. elegans* zygotic cell polarization, such as the CDC-42, LGL-1, and, CHIN-1 [Kumfer et al., *Mol. Biol. Cell*, 2010; Sailer et al., *Dev. Cell*, 2015; Beatty et al., *Development*, 2010]. The addition of these players increases the complexity of the cell polarity network tremendously, not only because of the explosion of the associated kinetic parameters, but also their role in related cellular processes such as cytoskeleton organization and localization at the poles that determines cell division dynamics [Ajduk et al., *Mol. Hum. Reprod.*, 2016; Lim et al., *Cell Rep.*, 2021]. Therefore, a more general understanding of the stability and asymmetry of cell polarization patterns will help to streamline experimental data analysis and interpretation. In a separate development, the theoretical knowledge acquired from nature is urgently needed for *de novo* construction of cells with designated characteristics, where the capability of cell polarization has been a design target since over a decade ago [Lin et al., *Nat. Commun.*, 2021; Watson et al., *Cell*, 2023; Tostevin et al., *Biophys J*, 2008; Chau et al., *Cell*, 2012].

In this work, we focus on the generation of stable asymmetric patterns in both the widely-used 2-node network and a more realistic *C. elegans* 5-node network. Starting from a symmetric antagonistic network, a polarized pattern can be stabilized at any interface location between the two antagonistic domains when translational symmetry is assumed. Unbalanced modification of kinetic parameters triggers movement of the interface in favor of one of the coexisting domains. There are three types of such unbalanced modification: single-sided self-regulation, single-sided additional regulation, and unequal system parameters. Nevertheless, the combination of two or more unbalanced modifications can recover pattern stability through fine-tuning of kinetic parameters. Alternatively, we show that the interface can also be stabilized at a designated location with a step-like spatial profile of one or more of the kinetic parameters, with values leading to opposing velocities when the interface is displaced. Intriguingly, such a program strategy is found to be employed in the *C. elegans* cell polarization network to maintain pattern stability along with considerable parameter robustness, while inducing pattern asymmetry by interface localization control.

2. Results

2.1 A computational pipeline for simulating cell polarization

To investigate both the simple network and the realistic network consisting of various node numbers and regulatory pathways [Goehring et al., *Science*, 2011; Lang et al., *Development*, 2017], we propose a computational pipeline for numerical exploration of the dynamics of a given reaction-diffusion network's dynamics, specifically targeting the maintenance phase of stable cell polarization after its initial establishment [Motegi et al., *Nat. Cell Biol.*, 2011; Goehring et al., *Science*, 2011; Seirin-Lee et al., *Cells*, 2020]. Numerous biological experiments on different organisms have demonstrated that such a reaction-diffusion network typically comprises

two groups of molecular species. Each group, once associated with a part of the cell membrane from the cell cytosol, inhibits the association of the other group in the same region, thereby creating two types of distinct domains [Knoblich et al., *Nat. Rev. Mol. Cell Biol.*, 2001; Doe et al., *Curr. Opin. Cell Biol.*, 2001]. At the interface between the two domains, the membrane association of proteins in either group is compromised due to the elevated level of antagonists. Nevertheless, one of the domains may expand at the expense of the other, leading to a finite interface velocity in general. For simplicity, three assumptions previously used in research are adopted to establish a reaction-diffusion model to describe the dynamics of each molecular species (denoted by [X]) during cell polarization:

1. The cellular space is reduced to a one-dimensional line of length L = 0.5, where x =−0.25 (anterior, where the concentration of molecular species accumulated on the cell membrane is denoted by [A_m]) and 0.25 (posterior, where the molecular species accumulated on the cell membrane is denoted by [P_m]) are its two poles (**Fig. 1a**) [Gross et al., *Nat. Phys.*, 2019; Seirin-Lee, *Dev. Growth Differ.*, 2020].
2. A molecular species of type [X] can associate with the cell membrane from cell cytosol at a rate $F_{\mathrm{on}}^{\mathrm{X}}(x,t)$ and dissociate from the cell membrane into cell cytosol at a rate $F_{\mathrm{off}}^{\mathrm{X}}(x,t)$, where t represents time. Both rates include leaky term and regulatory pathways affected by other molecular species [Seirin-Lee et al., *J. Theor. Biol.*, 2015; Seirin-Lee et al., *Cells*, 2020].
3. Based on previous experimental measurements, it has been reported that the diffusion rate of molecular species involved in cell polarization (*i.e.*, PAR-2 and PAR-6) is two orders of magnitude higher in the cell cytosol compared to the cell membrane [Goehring et al., *J. Cell Biol.*, 2011; Lim et al., *Cell Rep.*, 2021]. Consequently, we adopted 2.748×10^{-5} and 1.472×10^{-5} from previous research (nondimensionalized based on experimental measurements [Goehring et al., *J. Cell Biol.*, 2011; Goehring et al., Science, 2011; Seirin-Lee et al., *Cells*, 2020], as diffusion coefficients of anterior and posterior molecular species, while the cytoplasmic molecules are regarded as well-mixed with infinite diffusion [Kravtsova et al., *Bull. Math. Biol.*, 2014; Gross et al., *Nat. Phys.*, 2019; Morita et al., *J. Math. Biol.*, 2021]. We further assume that these molecular species are sufficiently abundant in the pool of cell cytosol, where the concentration is conserved as constant [X_c], although the analysis below can be extended to the more general case [Kravtsova et al., *Bull. Math. Biol.*, 2014; Goehring et al., *Science*, 2011].

For the concentration of each molecular species [X] on the cell membrane [X_m], the evolution equation is described by:

$$\frac{\partial[\mathrm{X_m}]}{\partial t} = D_{\mathrm{m}}^{\mathrm{X}}\frac{\partial^2}{\partial x^2}[\mathrm{X_m}] + F_{\mathrm{on}}^{\mathrm{X}}(x,t)[\mathrm{X_c}] - F_{\mathrm{off}}^{\mathrm{X}}(x,t)[\mathrm{X_m}], \tag{1}$$

where $D_{\mathrm{m}}^{\mathrm{X}}$ is the diffusion coefficient of molecular species [X] on the cell membrane. The first term on the right side represents the diffusion across the cell membrane; the second term represents the association with the cell membrane from the cytosol; while the third term represents the dissociation from the cell membrane into the cytosol. These regulated association and dissociation are given by the Hill equation [Seirin-Lee et al., *J. Theor. Biol.*, 2015; Seirin-Lee, *Bull. Math. Biol.*, 2021]:

$$F_{\mathrm{on}}^{\mathrm{X}}(x,t) = \gamma_{\mathrm{X}} + \sum_{\mathrm{Y}}\frac{q_{\mathrm{Y2}}^{\mathrm{X}}[\mathrm{Y_m}]^{n_{\mathrm{Yq}}^{\mathrm{X}}}}{1 + q_{\mathrm{Y1}}^{\mathrm{X}}[\mathrm{Y_m}]^{n_{\mathrm{Yq}}^{\mathrm{X}}}}, \tag{2}$$

$$F_{\mathrm{off}}^{\mathrm{X}}(x,t) = \alpha_{\mathrm{X}} + \sum_{\mathrm{Y}}\frac{k_{\mathrm{Y2}}^{\mathrm{X}}[\mathrm{Y_m}]^{n_{\mathrm{Yk}}^{\mathrm{X}}}}{1 + k_{\mathrm{Y1}}^{\mathrm{X}}[\mathrm{Y_m}]^{n_{\mathrm{Yk}}^{\mathrm{X}}}}, \tag{3}$$

where $F_{\mathrm{on}}^{\mathrm{X}}$ consists of a basal on-rate (*i.e.*, association rate) Υ_{X} and recruitment by other membrane-bound molecular species (Y ≠ X) and itself (Y = X, *i.e.*, self-activation), quantified by positive parameters $q_{\mathrm{Y}i}^{\mathrm{X}}\ (i=1,2)$; $F_{\mathrm{off}}^{\mathrm{X}}$ consists of a basal off-rate (*i.e.*, dissociation rate) α_{X} and exclusion by other molecular species (Y ≠ X) and itself (Y = X, *i.e.*, self-inhibition), quantified by positive parameters $k_{\mathrm{Y}i}^{\mathrm{X}}\ (i=1,2)$; the Hill coefficients $n_{\mathrm{Yq}}^{\mathrm{X}}$ and $n_{\mathrm{Yk}}^{\mathrm{X}}$ are set to 2 as used before [Seirin-Lee et al., *J. Theor. Biol.*, 2015; Seirin-Lee, *Bull. Math. Biol.*, 2021]. To simplify the model for numerical exploration with an affordable computational cost, we set the same responsive concentration $q_{\mathrm{Y}1}^{\mathrm{X}}=k_{\mathrm{Y}1}^{\mathrm{X}}=k_1$ for both activation and inhibition pathways; the inhibition intensities $k_{\mathrm{Y}2}^{\mathrm{X}}$ are set to 1 as a numerically normalized value. We also set self and mutual activation parameters $q_{\mathrm{Y}2}^{\mathrm{X}}=q_2$ to be the same for synergistic proteins in the same group. Finally, the basal association and dissociation rates are regarded the same so that these spatially-independent effects can be neutralized, in other words, $\Upsilon_{\mathrm{X}}=\alpha_{\mathrm{X}}=\Upsilon$. Consequently, there are only three independent parameters governing this system: Υ, k_1, and q_2. A detailed description of the parameters is listed in Table S1. This dimensionally reduced parameter configuration is sufficient to describe the temporal evolution of polarization distribution on the membrane under the well-mixed cytoplasmic protein concentration. All the simplified parameter value assignments above will be extensively explored by giving different values to different molecular species and pathways as well as setting a heterogeneous spatial distribution.

Simulations are performed by systematically scanning the dimensionless parameter set Ω(Υ, k_1, q_2) on a three-dimensional (3D) grid Υ∈ [0,0.05] in steps ΔΥ = 0.001, k_1 ∈ [0,5] in steps Δk_1 = 0.05, and q_2 ∈ [0,0.05] in steps Δq_2 = 0.001. The derived nondimensionalized parameter attains values on the same order of magnitude as those observed in reality, confirming the fidelity of the proposed model in representing the real system (Supplemental Text). When it comes to a statement of switch from pattern stability to instability, the three-parameter simplification will be removed to free the parameter value assignments (*i.e.*, uniform random variables Υ ∈ [0,0.05], α ∈ [0,0.05], k_1 ∈ [0,5], q_2 ∈ [0,5], q_1 ∈ [0,5], q_2 ∈ [0,0.05], and $[\mathrm{X_c}]$ ∈ [0.05,5] added for setting up a network with cell polarization pattern stability, searched by the Monte Carlo method) concerning all nodes and regulations, auxiliarily validating the conclusion [Fishman, *Springer New York*, 1995].

Focusing on the stability and asymmetry of cell polarization during the maintenance phase, we simplify and set the initial distribution of molecular species on the cell membrane, $[\mathrm{X_m}](x,0)$, which is polarized during the establishment phase through active actomyosin contractility and flow [Munro et al., *Dev. Cell*, 2004; Kravtsova et al., *Bull. Math. Biol.*, 2014], using the sigmoid function:

$$\begin{cases}[\mathrm{X_m}](x,0)=1-\dfrac{1}{1+e^{-20x}}, & \text{for anterior molecular species}\\ [\mathrm{X_m}](x,0)=\dfrac{1}{1+e^{-20x}}, & \text{for posterior molecular species}\end{cases}. \tag{4}$$

Then the set of partial differential equations (1) evolves for 500 steps with a time step of 1 (Fig. S1). The solution at t = 500 is saved for further analysis if:

1. All the molecular species still have a polarized pattern, as defined by $[\mathrm{X_m}](x=-L/2,\ t=500) > 0.5$ and $[\mathrm{X_m}](x=L/2,\ t=500) < 0.5$ for the anterior molecular species and $[\mathrm{X_m}](x=-L/2,\ t=500) < 0.5$ and $[\mathrm{X_m}](x=L/2,\ t=500) > 0.5$ for the posterior molecular species.
2. The cell polarization pattern is stable or nearly intact over time for each molecular species, as defined by
$$\left|\frac{[\mathrm{X_m}](x_0,\ t=500)-[\mathrm{X_m}](x_0,t=499)]}{[\mathrm{X_m}](x_0,t=499)}\right|<10^{-4}, x_0\in[-0.25,0.25] \tag{5}$$

Implemented on *Matlab* 2022b [The MathWorks Inc., 2022b], such a computational pipeline can describe the spatiotemporal dynamics of any reaction-diffusion network design, for evaluating its capability of maintaining cell polarization (Fig. S1). Meanwhile, we construct an automatic software, *PolarSim*, for users to explore networks with arbitrarily set node numbers, parameter values, and regulatory pathways (Supplemental Text).

2.2 An unbalanced network structure or parameter leads to the collapse of a polarized pattern

Previous experimental and theoretical discoveries have uncovered the mutual inhibition between two molecular species as a fundamental design capable of generating cell polarization [Kemphues et al., *Cell*, 1988; Cuenca et al., *Development*, 2003; Tostevin et al., *Biophys. J.*, 2008; Chau et al., *Cell*, 2012]. Thus, we utilize the completely symmetric antagonistic 2-node network to investigate the behavior of its cell polarization pattern when the network structure or parameter is modified. The two nodes (*i.e.*, molecular species) placed in the anterior and posterior are denoted by [A] and [P]. As there is no activation here then q_2 is not considered, the computational pipeline above establishes a total of 122 viable parameter sets (Υ, k_1) (~2.37% among 5,151 sets) that can achieve stable cell polarization. We use (Υ = 0.05, k_1 = 0.05) as a representative to show how the corresponding cell polarization pattern behaves under alternative initial condition and elementary modification (**Fig. 1**, Fig. S2).

Regarding the initial conditions, while uniform initial distributions maintain a homogeneous pattern (Fig. S2a, b), a polarized initial distribution reliably maintains the cell polarization regardless of variations in the initial distribution, such as shifts in transition planes (Fig. S2c, d), weak polarization (Fig. S2e, f), or asymmetric curve shapes between the two molecular species (Fig. S2f, g). In contrast, an initial distribution with only Gaussian noise produces a multipolar pattern, with the two molecular species still locally excluding each other (Fig. S2h). Altogether, these findings demonstrate the necessity of additional mechanisms, such as the active actomyosin contractility and flow, for establishing initial cell polarization independently of the reaction-diffusion network during the establishment phase [Cuenca et al., *Development*, 2003; Gross et al., *Nat. Phys.*, 2019].

Regarding the elementary modification, a total of three types are exerted on the node [A]:

1. Single-sided self-regulation (**Fig. 1b**): a self-activation ($q_{\mathrm{A2}}^{\mathrm{A}} = 0.012$) or self-inhibition ($k_{\mathrm{A2}}^{\mathrm{A}} = 0.1$) is added on the node [A].
2. Single-sided additional regulation (**Fig. 1c** and Fig. S3): a new node [L] is added in the anterior or posterior, with mutual activation ($q_{\mathrm{L2}}^{\mathrm{A}}$ & $q_{\mathrm{A2}}^{\mathrm{L}} = 0.012$) or inhibition ($k_{\mathrm{L2}}^{\mathrm{A}} = k_{\mathrm{A2}}^{\mathrm{L}} = 0.025$) with [A]. The location of the additional node [L] decides the initial polarized pattern represented by the sigmoid function, where an anterior node starts with a high concentration in the anterior and a low concentration in the posterior, and vice versa.
3. Unequal system parameters (**Fig. 1d**): on one hand, the inhibition intensity k_2 from [P] to [A] is increased from 1 to 1.6; on the other hand, the cytoplasmic concentration of [A] is increased from 1 to 1.25. The other system parameters (*e.g.*, basal on-rate Υ and basal off-rate α) will be explored independently in the next section.

In comparison with the stable cell polarization pattern generated by the basic network, the protein distribution dynamics of eight modified conditions are simulated as shown in **Fig. 1** and Movie S1, where the domain of one molecular species keeps invading the domain of the other one, ending in a homogeneous distribution. Such pattern instability caused by unbalanced network modification still holds when the network is initially set up using different initial conditions and parameters (*i.e.*, Υ, α, k_1, k_2, and $[\mathrm{X_c}]$) assigned with various values concerning all nodes and

regulations (Fig. S4, Fig. S5 - 1st row, and Table S1). This intuitively reveals that the antagonistic 2-node reaction-diffusion network is prone to become unstable with its interface keeps moving when the perturbation is introduced to the network structure or parameter.

2.3 The combination of two modifications can recover the cell polarization pattern stability

Since a single modification of reaction-diffusion network structure or parameter is enough to break the cell polarization pattern, an appealing question just comes up: how can the network be designed to maintain pattern stability considering such modifications? This is crucial for cell polarization in reality where stability is essential for cell function and survival; without stability, the spatial information defined by the pattern is inaccurate for guiding downstream biological events such as cell division and cell differentiation [Hubatsch et al., *Nat. Phys.*, 2019; Wang et al., *Adv. Exp. Med. Biol.*, 2013]. The simplest idea for stability recovery is to combine two kinds of modifications with opposite trends, for example, adding self-activation and posteriorly inhibition on [A] simultaneously. For the three types of modification, we arbitrarily select one subtype within each of them from **Fig. 1b-d** so three combinatorial networks are constituted, all of whose interfaces turn out to be stabilized finally (**Fig. 2** and Movie S2).

To more precisely elucidate how two opposite modifications coordinate the pattern stability together, we make use of the network with self-activation and additional inhibition on [A] (shown in the top right corner of **Fig. 2**), where the two corresponding intensities $q_{\mathrm{A2}}^{\mathrm{A}}$ and $k_{\mathrm{L2}}^{\mathrm{A}}$ & $k_{\mathrm{A2}}^{\mathrm{L}}$ compose a phase diagram that distinguishes the final state of the reaction-diffusion pattern. The moving velocity of the pattern is defined as follows:

$$v(t)=\frac{1}{N}\sum_{\mathrm{X}}\frac{\int_{-\frac{L}{2}}^{\frac{L}{2}}|[\mathrm{X_m}](x,t)-[\mathrm{X_m}](x,t-1)|\,\mathrm{d}x}{L}. \tag{6}$$

where N is the total number of the molecular species. Here, we classify the final state by calculating the moving velocity of the pattern at the final time t = 500; the region with $v < 10^{-4}$ around the diagonal line is marked as the polarized state, while the regions upon and beneath it are homogeneous states dominated by [A] and [P] respectively (**Fig. 3a**). Therefore, the triphase diagram and the exemplary patterns generated by the parameter assignments ①②③ shown in **Fig. 3a** suggest the necessity of the balance between two opposite modifications for setting up a stable cell polarization pattern.

Apart from the unequal inhibition intensity and cytoplasmic concentration mentioned in **Fig. 2d**, we further ask if all the kinetic parameters with biophysical significance (including inhibition intensity k_2, responsive concentration k_1, basal on-rate ϒ, basal off-rate α, and cytoplasmic concentration [$\mathrm{X_c}$]) also require a balance for achieving pattern stability. For this purpose, we generate the phase diagrams between each of them and the inhibition intensity $k_{\mathrm{A2}}^{\mathrm{P}}$. Fascinatingly, monotonic correlations exist between all those system parameters, suggesting that they can be tuned to maintain pattern stability (**Fig. 3b**). In the grey region, the symmetric-broken parameters can be weighed against each other to realize the interface velocity close to zero.

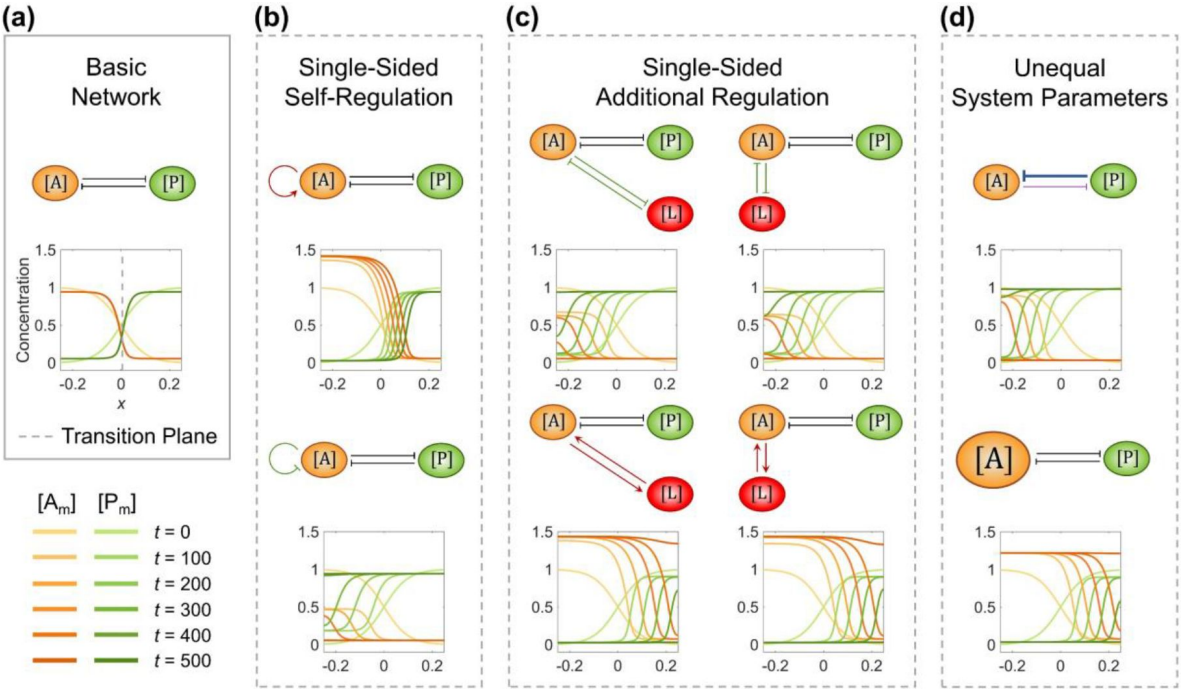

Fig. 1.

The single modification on the antagonistic 2-node network causes the collapse of the cell polarization pattern.

(a) Basic network with the transition plane marked by grey dashed line.(b) Two subtypes of single-sided self-regulation. (c) Four subtypes of single-sided additional regulation. The corresponding spatial concentration distribution of $[L_m]$ at t = 0, 100, 200, 300, 400, and 500, and the subtle difference between left and right panels are detailed in Fig. S3. (d) Two subtypes of unequal system parameters, exemplified by unequal inhibition intensity and unequal cytoplasmic concentration. For each network, the corresponding spatial concentration distribution of $[A_m]$ and $[P_m]$ at t = 0, 100, 200, 300, 400, and 500 are shown beneath with a color scheme listed in the bottom left corner. Note that within a network, normal arrows and blunt arrows symbolize activation and inhibition respectively.

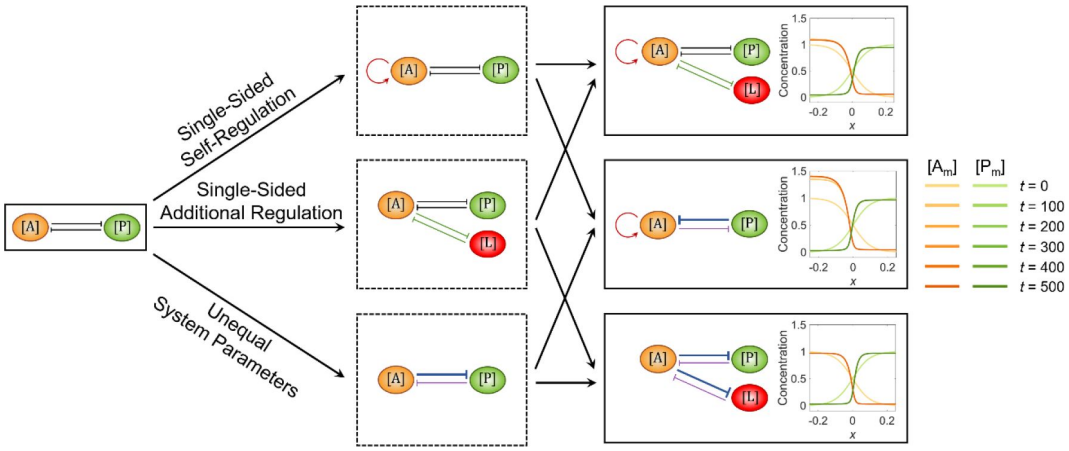

Fig. 2.

The combination of two opposite modifications recovers the stability of the cell polarization pattern.

The basic network and the ones added with a single modification are shown in the 1st and 2nd columns respectively; the three combinatorial networks composed of any two of the three single modifications are shown in the 3rd column. For each network, the corresponding concentration distribution of $[A_m]$ and $[P_m]$ at t = 0, 100, 200, 300, 400, and 500 are shown beneath with a color scheme listed on the right. Here, the value assignments on the modifications in the 3rd column are as follows: $q^{A}_{A2} = 0.012$ and k^{A}_{L2} & $k^{L}_{A2} = 0.01$ for 1st row, $q^{A}_{A2} = 0.012$ and $k^{A}_{P2} = 1.24$ for 2nd row, and $q^{A}_{A2} = 0.012$ and k^{P}_{A2} & $k^{L}_{A2} = 2$ for 3rd row. Note that within a network, normal arrows and blunt arrows symbolize activation and inhibition respectively.

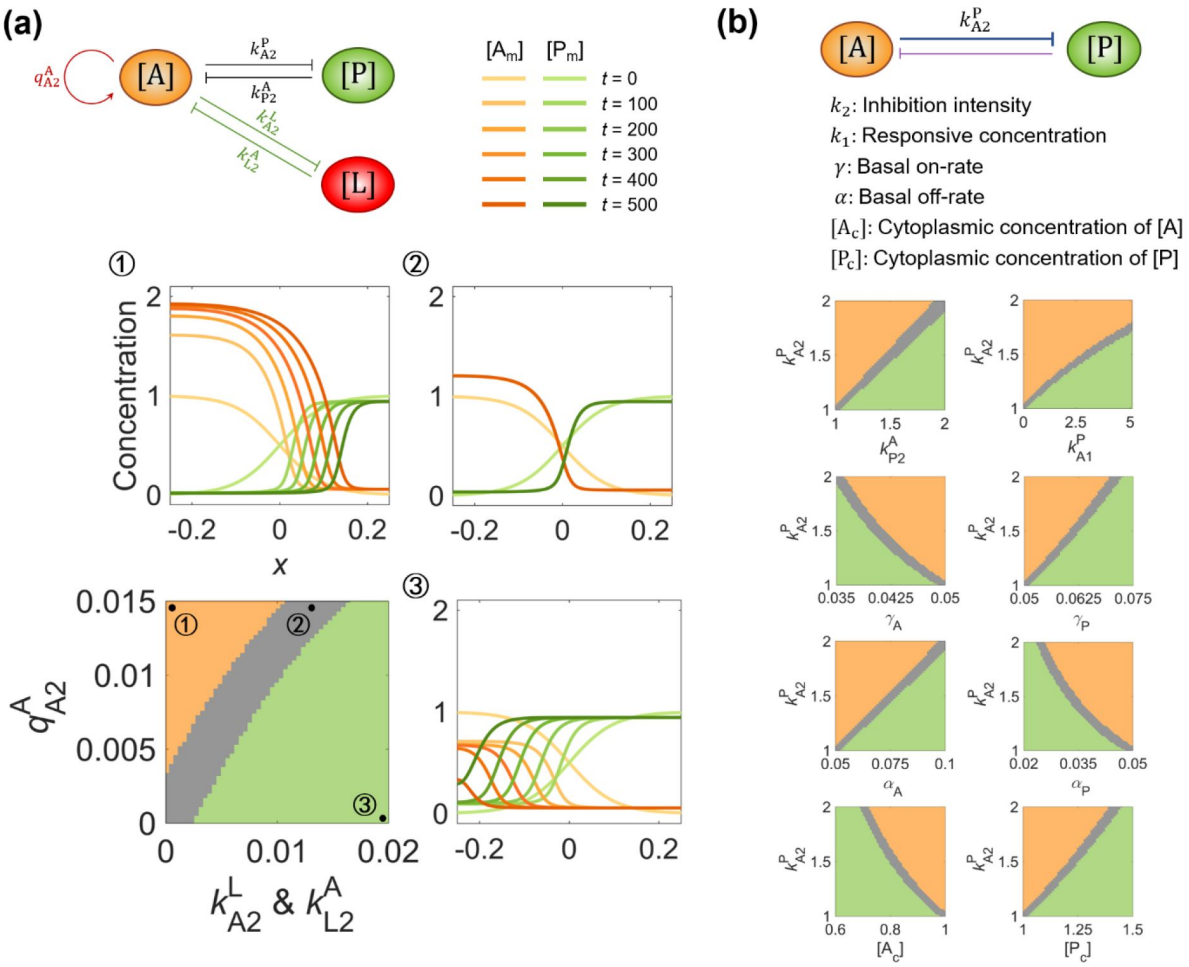

Fig. 3.

The balance between system parameters is needed for maintaining pattern stability.

(a) The phase diagram between q^{A}_{A2} and k^{A}_{L2} & k^{L}_{A2} in the network modified by self-activation (quantified by q^{A}_{A2}) and additional inhibition (quantified by k^{A}_{L2} & k^{L}_{A2}) on [A]. The representative parameter assignment for each phase are marked with ① (*i.e.*, $q^{A}_{A2} = 0.015$ and k^{A}_{L2} & $k^{L}_{A2} = 0$ with a homogeneous state dominated by [A]), ② (*i.e.*, $q^{A}_{A2} = 0.015$ and k^{A}_{L2} & $k^{L}_{A2} = 0.0135$ with a stable polarized state), and ③ (*i.e.*, $q^{A}_{A2} = 0.02$ and k^{A}_{L2} & $k^{L}_{A2} = 0$ with a homogeneous state dominated by [P]). The corresponding concentration distribution of [A_m] and [P_m] at *t* = 0, 100, 200, 300, 400, and 500 are shown around the phase diagram with a color scheme listed on top. (b) The phase diagram between responsive concentration k_1, basal on-rate Y, basal off-rate α, cytoplasmic concentration [X_c], and inhibition intensity k_2. For each phase diagram in (a)(b), the final state dominated by [A] or [P] or stable polarized is colored in orange, green, and gray, respectively. Note that within a network, normal arrows and blunt arrows symbolize activation and inhibition respectively.

2.4 The velocity and position of the interface can be adjusted by setting up spatial cues

The required balance between parameters provides insight into controlling the pattern stability. However, in biological organisms, there exists influence from cellular actomyosin flow and extracellular/intercellular signals, leading to changeable molecular concentration and parameter values in different parts of space [Arata et al., *Development*, 2010; Beatty et al., *Development*, 2013]. How do cells maintain cell polarization pattern stability in the case of nonuniform initial conditions and parameter values, namely finding zero-velocity solutions at interfaces? Here, given a specific pattern, its position of transition plane or interface $x_T(t)$ is defined by the mean position of all the molecular species where the absolute derivative value of the concentration curve reaches its maximum.

First, based on the symmetric 2-node network ($\Upsilon = 0.05$, $k_1 = 0.05$, **Fig. 4a**, the same simulation as the one in **Fig. 1a**), we alter its initial condition by shifting the interface position or exerting a homogeneous or Gaussian noise distribution without any positional information (Fig. S2); it is found that the initial polarized pattern is essential for constricting only one single interface with predetermined position, while the homogeneous or Gaussian noise distribution results in no or multiple interfaces (Fig. S2a, b, h). This indicates the importance of additional mechanisms (*e.g.*, the cortical flow on the cell membrane that transports proteins related to cell polarity) establishing the initial cell polarization pattern before the pattern enters the maintenance phase, when the network structure and parameters account for its stability in the long term [Cuenca et al., *Development*, 2003; Motegi et al., *Nat. Cell Biol.*, 2011].

Next, to probe into how nonuniform biophysical parameter values can control the interface in concert, we employ the following adjustment on the parameter set used in **Fig. 4a**:

1. Increasing the inhibitory intensity of [A] on [P], k_{A2}^{P}, from 1 to 1.5, leads to the interface continuously shifting to the posterior, and [A] finally dominates.
2. Reducing the basal on-rate of [A], Υ_A, from 0.05 to 0.01, results in the interface moving to the anteriority, and [P] finally dominates.

When these two systems are combined, the stable polarity pattern remains with (i) used in the region $x < 0$ while (ii) used in $x > 0$ (**Fig. 4b**). By moving the step position of the parameter function to $x = -0.1$ (**Fig. 4c**) and $x = 0.1$ (**Fig. 4d**), the interface stabilizes around the step, which means the interface position is tunable (Movie S3). This indicates that by using parameter sets with values corresponding to opposite interface velocities on two sides of the interface, the interface velocity and position of the polarity pattern can be precisely regulated. The nonuniform spatial distribution of parameters imitates signaling perception, which provides a strategy for more robust control of the adjustable interface position in response to variable cues.

2.5 Reconstruction of the molecular interaction network and the design principle of parameter trade-off in C. elegans zygote

In the 2-node network, the cell polarization pattern stability could be broken by a single modification (**Fig. 1**) and recovered by two combinatorial modifications (**Fig. 2**, **Fig. 3**), or with the zero-velocity interface position regulated by spatially inhomogeneous parameters (**Fig. 4**). We further ask if such a fundamental rule is employed in the cell polarization network programming in a real system. To this end, we focus on the zygote of the nematode *C. elegans*, which has been a popular model for cell polarization study from both experimental and theoretical perspectives for more than 3 decades [Kemphues et al., *Cell*, 1988; Lang et al.,

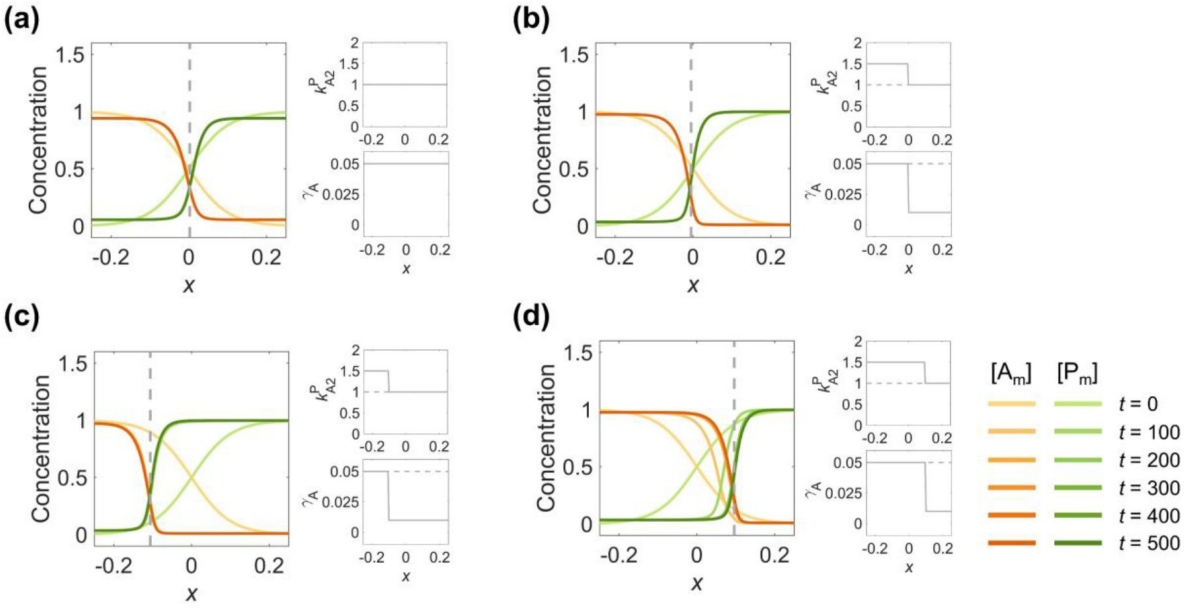

Fig. 4.

Adopting parameter sets corresponding to opposite interface velocities on two sides of the interface, the zero-velocity interface position of the polarity pattern is shifted and regulatable.

(a) Spatially uniform parameters (2nd column) of a symmetric 2-node network generate a symmetric pattern (1st column), from the same simulation in **Fig. 1a**. (b) Using the parameter combination with the posterior-shifting interface on the left and anterior-shifting interface on the right, a stable polarity pattern (1st column) can be remained by increasing k_{A2}^{P} to 1.5 at $x < 0$ and decreasing Y_A to 0.01 at $x > 0$ (2nd column). (c-d) The stable interface position can be optionally adjusted by setting the change position of the step-up function (2nd column). (c) As in (b), but changing the step position to $x = -0.1$, the interface stabilizes around $x = -0.1$ (1st column). (d) As in (b), but changing the step position to $x = 0.1$, the interface stabilizes around $x = 0.1$ (1st column). For each parameter set, the corresponding spatial concentration distribution of $[A_m]$ and $[P_m]$ at $t = 0$, 100, 200, 300, 400, and 500 are shown beneath with a color scheme listed on the right. Note that all the interface positions in (b-d) are marked by the vertical dashed line in gray.

Development, 2017; Goehring et al., *Science*, 2011; Lim et al., *Cell Rep.*, 2021]. By conducting an exhaustive literature search (a total of 19 references), we summarize the mutual interaction network in *C. elegans* zygote that consists of five interacting molecular species: PAR-3/PAR-6/PKC-3 complex (*abbr.*, [A]) and CDC-42 protein (*abbr.*, [C]) accumulated in the anterior, and PAR-1/PAR-2 complex (*abbr.*, [P]), LGL-1 (*abbr.*, [L]), and CHIN-1 (*abbr.*, [H]) accumulated in the posterior (**Fig. 5a**). The detailed description of the biochemical mechanism of each regulatory pathway as well as the corresponding supporting references are listed in Table S2. Based on the network obtained experimentally, the computational pipeline described in **Section 2.1** establishes a total of 602 viable parameter sets (Y, k_1, q_2) (~0.229% among 262,701) that can achieve stable cell polarization (**Fig. 5d, e**).

To verify whether the computational pipeline is reliable enough to simulate the dynamics of protein distribution of the *C. elegans* network *in vivo*, we further reproduce a series of perturbation experiments reported previously. It's worth noting that the reconstructed *C. elegans* 5-node network appears to be an integration of an antagonistic 2-node network doubled into an antagonistic 4-node network (**Fig. 5b**) with full connections, and the [A]~[C] mutual activation (**Fig. 5c**) and [A]~[L] mutual inhibition (**Fig. 5d**). As the antagonistic 2-node network has been revealed to be a fundamental structure capable of stable cell polarization [Tostevin et al., *Biophys J*, 2008; Goehring et al., *Science*, 2011; Chau et al., *Cell*, 2012], hereafter we focus on how the added interactions involved with [C] (the protein accumulated in the anterior and with an additional mutual activation with [A] in the anterior) and [L] (the protein accumulated in the posterior and with an additional mutual inhibition with [A] in the anterior) impact the pattern stability concordantly (Fig. S6).

Taking [L] as the first example for its current absence of theoretical model analysis [Seirin-Lee et al., *Cells*, 2020, Lim et al., *Cell Rep.*, 2021], a series of experimental groups in different conditions were conducted before by knocking down or overexpressing [L], followed by a measurement of the lethality in embryo individuals (defined by death rate and proven to be a consequence of polarity loss in the zygote, which is essential for asymmetric cell division and cell differentiation) [Beatty et al., *Development*, 2010; Beatty et al., *Development*, 2013; Rodriguez et al., *Dev. Cell*, 2017; Jankele et al., *eLife*, 2021]. Here, we utilize the pattern error in a mutant (*abbr.*, MT) embryo compared to the wild-type (*abbr.*, WT) one,

$$\text{Error} = \frac{1}{M}\sum_{i=1}^{M}\frac{\int_{-\frac{L}{2}}^{\frac{L}{2}}|[\mathrm{X_m}]_{\mathrm{WT}}(x,t=500)-[\mathrm{X_m}]_{\mathrm{MT}}(x,t=500)|\mathrm{d}x}{L}$$

, to represent level of polarity loss in simulation and lethality in experiment (measured from previous literature), where M = 602 is the number of viable parameter sets (~0.229% among 262,701). The first group of experiments is that the double depletion on [P] and [L] leads to much more lethality than single depletion on either [P] or [L], which is recapitulated by Fig. S7a, b (cell polarization pattern characteristics in simulation: larger pattern error in double depletion on [P] and [L], compared to single depletion on either [P] or [L]) [Hoege et al., *Curr. Biol.*, 2010]. The second group of experiments is that the overexpression of [L] lowers the lethality induced by single depletion on [P] and such effect is weakened when [H] is depleted as well, which is recapitulated by Fig. S7c, d (cell polarization pattern characteristics in simulation: smaller pattern error in single depletion on [P] supplemented by overexpression of [L], compared to single depletion on [P] only; less smaller pattern error in double depletion on [P] and [L] supplemented by overexpression of [L], compared to single depletion on [P] only) [Beatty et al., *Development*, 2010; Beatty et al., *Development*, 2013].

The second example of theoretical model analysis involves [C]. A series of experimental groups in different conditions were conducted before by knocking down or overexpressing [C] or blocking the mutual activation between [A] and [C], followed by an observation of the pattern polarity in embryo individuals. The first group of experiments is that the single depletion on [C] results in polarity defects and the mislocalization of PAR-6 and PAR-2, which is recapitulated by Fig. S8a, b

(cell polarization pattern characteristics in simulation: less polarized distributions of [A] and [P], compared to WT) [Gotta et al., *Curr. Biol.*, 2001; Aceto et al., *Dev. Biol.*, 2006]. The second group of experiments is that the overexpression of [C] increases the size of the anterior domain, which is recapitulated by Fig. S8a, c (cell polarization pattern characteristics in simulation: posteriorly shifted interfaces of [A] and [P], compared to WT) [Aceto et al., *Dev. Biol.*, 2006]. The third group of experiments is that blocking the interaction between PAR-6 and CDC-42 results in polarity defects very similar to those associated with single depletion on CDC-42, which is recapitulated by Fig. S8a, d (cell polarization pattern characteristics in simulation: less polarized distribution of [A] in both conditions, compared to WT) [Aceto et al., *Dev. Biol.*, 2006].

To sum up, apart from the cell polarization in a wild-type embryo, our modeling framework is further validated by reproducing two groups of perturbation experiments that haven't been theoretically explained before, allowing further computational investigation of the network dynamics.

With the well-validated model of the *C. elegans* cell polarization network, here we study if it follows the balance design revealed by the exhaustive study on the antagonistic 2-node network. Interestingly, the central structure of the *C. elegans* network is shown to be a completely symmetric network composed of 2 nodes in the anterior (*i.e.*, [A] and [C]) and posterior (*i.e.*, [P] and [H]) respectively; this symmetric 4-node network is modified by a mutual activation in the anterior (*i.e.*, [A]~[C]) firstly and an additional mutual inhibition between the anterior and the posterior (*i.e.*, [A]~[L]) subsequently, turning into an asymmetric 5-node network (**Fig. 5b-d**). The abovementioned symmetric structure, the mutual activation, and the additional inhibition are in analogy with the basic 2-node network modified by self-activation and additional inhibition as shown in the top right corner of **Fig. 2** and **Fig. 3a**.

Here, we seek to compare the concentration distribution and moving velocity of the patterns generated by the three successive network structures termed "4-Node" (the symmetric structure) (**Fig. 5b**), "LGL-1$^-$" (the symmetric structure with [A]~[C] added, *i.e.*, the mutant network with [A]~[L] depleted from the wild-type network) (**Fig. 5c**), and "WT" (the symmetric structure with both [A]~[C] and [A]~[L] added, *i.e.*, the wild-type network) (**Fig. 5d**). As expected, both simulations on the 4-Node and WT networks successfully pass the computation pipeline described in **Section 2.1** with 62 (~1.20% among 5,151) and 602 (~0.229% among 262,701) viable parameter sets respectively (**Fig. 5e**), all of which stabilize into a cell polarization pattern with the concentration distribution highly intact and the moving velocity of each parameter set continuously declining below 10^{-4} (**Fig. 5b**, d and Movie S4). Nonetheless, the intermediate one (generated by depleting [A]~[L] from the WT network) with [A]~[C] but without [A]~[L] fails (**Fig. 5c** and Movie S4), exhibiting a dispersed concentration distribution and stubbornly high moving velocity for its pattern. Such pattern instability caused by unbalanced network modification still holds when the network is initially set up using different initial conditions and parameters (*i.e.*, γ, α, k_1, k_2, q_1, q_2 and $[X_c]$) assigned with various values concerning all nodes and regulations (Fig. S5 - 2nd row, Fig. S9, Table S1), just like the simple 2-node network (Fig. S4, Fig. S5 – 1st row, Table S1). Therefore, WT shows the largest variable parameter sets in the limited 3D grid and the strongest stability among the three network structures.

Remarkably, the balance between these two modifications is required to achieve stable cell polarization (**Fig. 5f**). To evaluate how the interface moves, we quantify the interface velocity by the rate of the transition plane x_T with respect to time. To avoid the influence of the initial state, the interface velocity is then calculated as the average velocity from t = 300 to t = 500.

$$v_I = \frac{x_T(t = 500) - x_T(t = 300)}{200} \tag{7}$$

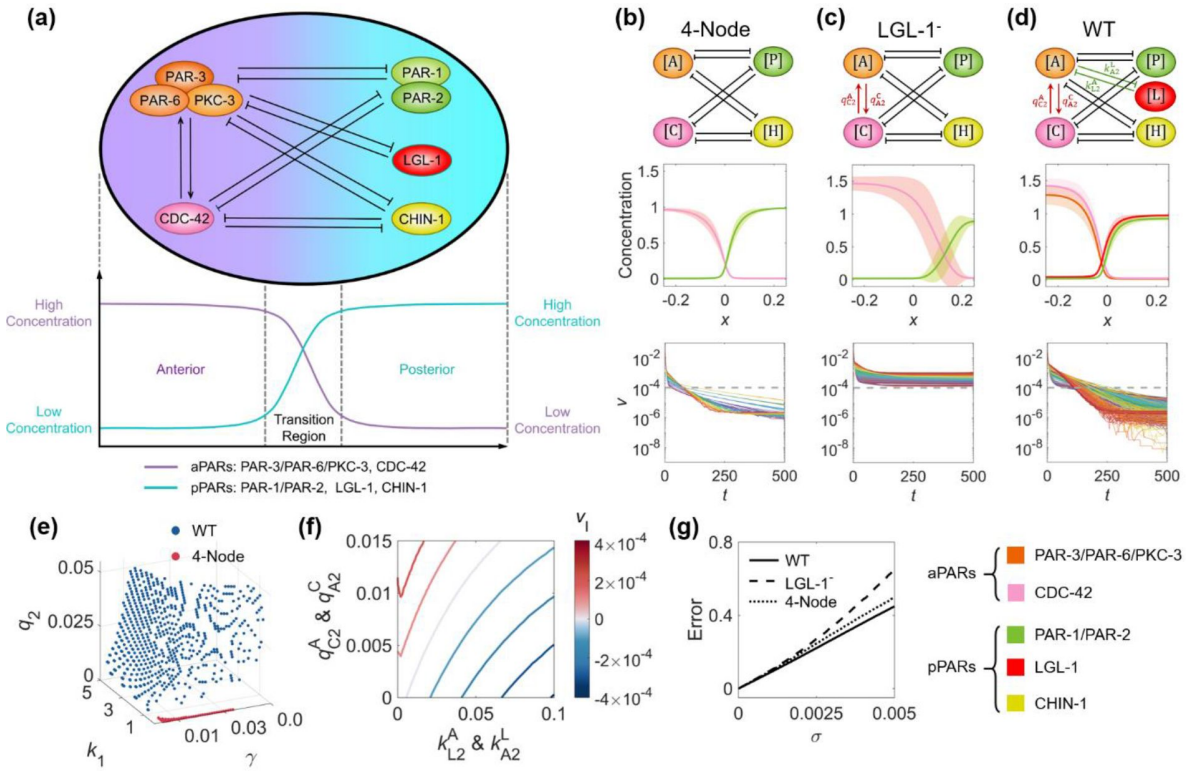

Fig. 5.

The molecular interaction network in *C. elegans* zygote and its natural advantages in terms of pattern stability, viable parameter sets, balanced network configuration, and parameter robustness.

(a) The schematic diagram of the network composed of five molecular species, each of which has a polarized spatial concentration distribution on the cell membrane shown beneath. The left nodes PAR-3/PAR-6/PKC-3 (*i.e.* [A]) and CDC-42 (*i.e.* [C]) exhibit high concentration in the anterior pole and low concentration in the posterior pole, schemed by the purple line beneath; the right nodes PAR-1/PAR-2 (*i.e.* [P]), LGL-1 (*i.e.* [L]), and CHIN-1 (*i.e.* [H]) exhibit low concentration in the anterior pole and high concentration in the posterior pole, schemed by the cyan line beneath. Note that within the network, normal arrows and blunt arrows symbolize activation and inhibition respectively. (b-d) The structure of 4-Node, LGL-1$^-$, and WT networks (1st row). The final spatial concentration distribution (t = 500) averaged over all established viable parameter sets for each molecular species (*i.e.*, 62 among 262,701 sets, ~0.024%, for the 4-Node network; 62 among 5,151 sets, ~1.2%, for the LGL-1$^-$ network; 602 among 262,701 sets, ~0.229%, for the WT network), shown by a solid line (2nd row). For each position, MEAN ± STD (*i.e.*, standard deviation) calculated with all viable parameter sets is shown by shadow. The moving velocity of the pattern (v) over evolution time (t) (3rd row). For each subfigure in 3rd row, each line with a unique color represents the simulation of a unique viable parameter set, and $v = 10^{-4}$ is marked by a dashed line. For (a-d), the legend for the relationship between molecular species and corresponding color is placed in the bottom right corner. (e) The viable parameter sets of WT (blue points; 602 viable solutions among 262,701 sets, ~0.229%) and 4-Node networks (red points; 62 viable solutions among 5,151 sets, ~1.20%). (f) The interplay between [A]~[C] mutual activation and [A]~[L] mutual inhibition on the interface velocity. The contour map of the interface velocity v_I with different parameter combinations of q_{C2}^{A} & q_{A2}^{C} and k_{L2}^{A} & k_{A2}^{L} represents its moving trend. The darker the red is, the faster the interface is moving toward the posterior pole; the darker the blue is, the faster the interface is moving toward the anterior pole; the closer the color is to white, the more stable the interface is. (g) The averaged pattern error in a perturbed condition compared to the original 4-Node, LGL-1$^-$, and WT networks. The Gaussian noise is simultaneously exerted on all the parameters Y, α, k_1, k_2, q_1 and q_2, where standard deviation σ denotes the noise amplification. For a specific noise level, the pattern error is averaged over 1000 independent simulations.

Scanning the intensities of [A]~[C] mutual activation (*i.e.*, q_{A2}^{C} & k_{C2}^{A}) and [A]~[L] mutual inhibition (*i.e.*, k_{A2}^{L} & k_{L2}^{A}), a contour map is shown in consideration of the interface velocity averaged over all viable parameter sets (*i.e.*, v_I): the system can be stably polarized when they are in balance with its interface velocity close to zero, but the overshoot of either intensity leads to a homogeneous state in the end (**Fig. 5f**). The redder the contour color is, the faster the interface moves posteriorly, with an increasing aPARs domain; the bluer the contour color is, the faster the interface moves anteriorly, with pPARs invading.

Next, we wonder if such combinatorial modifications may be an optimal choice selected during evolution. To this end, we regard the [A]~[C] mutual activation as a primary modification that induces pattern asymmetry as proposed before [Seirin-Lee et al., *Cells*, 2020; Lim et al., *Cell Rep.*, 2021], then the existence, as well as the form of the feed loops between [L] and a preexisting molecular species, is a supporting modification that consolidates stable polarization. Considering the symmetric structure of the LGL-1$^-$ network, there is an identical role between [A] and [C] and between [P] and [H], so [L] can be effectively connected to [A] or [P]; meanwhile, there are three types of directional regulation between them: activation, inhibition, and none. Thus, in theory, there are 32 possible network structures with an additional regulation, in which [L] must interact with one of the existing nodes (Fig. S10). Strikingly, only the WT network with mutual inhibition between [A] and [L] passes the computational pipeline with viable parameter sets. Thus, without any parametric asymmetry concessions, the configuration of the *C. elegans* network in nature is well optimized among all other alternatives for maintaining cell polarization pattern stability.

As pattern stability means how fast the pattern moves over time, does the lack of pattern stability result in a more dispersed concentration distribution when the system parameters fluctuate in time? To test this hypothesis, for each viable parameter set, we exert Gaussian noise on all the original values of system parameters Υ, α, k_1, k_2, q_1, and, q_2, and initiate 1000 independent simulations, where the noise amplification is represented by the standard deviation σ of the Gaussian noise [Guan et al., *Phys. Rev. E*, 2021]. To compare the variance of perturbed condition (*abbr.*, PT) to the original pattern (*abbr.*, OP, including, 4-Node, LGL-1$^-$, and WT), the pattern error, averaged over all molecular species, all the viable parameter sets, and all independent simulations, is defined as follows:

$$\text{Error} = \frac{1}{MQN}\sum_{i=1}^{M}\sum_{j=1}^{Q}\sum_{\mathrm{X}}\frac{\int_{-\frac{L}{2}}^{\frac{L}{2}}|[\mathrm{X_m}]_{\mathrm{OP}}(x,t=500)-[\mathrm{X_m}]_{\mathrm{PT}}(x,t=500)|\mathrm{d}x}{L} \tag{8}$$

where *M, Q, N* represents the number of the viable parameter sets (*i.e.* 602 (~0.229% among 262,701) for WT, 62 (~1.20% among 5,151) for 4-Node and 62 (~0.024% among 262,701) for LGL-1$^-$), independent simulations (*i.e.* 1000) and molecular species (*i.e.* five for WT, four for 4-Node and LGL-1$^-$). It turns out that the pattern error is always the smallest in the WT network and biggest in the LGL-1$^-$ network, no matter how strong the noise is, indicating parameter robustness as the companion advantage of pattern stability (**Fig. 5g**).

2.6 A protocol to identify responsive parameters for interface positioning

For a polarization pattern to be stable, fine-tuning of the kinetic parameters is required to reach the vanishing velocity of the pattern interface (numerically identified by **Eq. (5)**). Using the 5-node *C. elegans* network as an example, we outline a method to delineate iso-velocity surfaces $v_I(\Omega)$ = constant in the high-dimensional space of the parameter set Ω. We show that the information gained can be used to quantify the role of individual molecular components in controlling the polarized pattern. Additionally, this knowledge enables us to design experiments to produce desired patterns.

The method of iso-velocity surface delineation is outlined as the following. In **Sec. 2.5**, 602 (~0.229% among 262,701) groups of parameters capable of reaching stable polarity patterns are found by scanning through parameter space. When plotted in the three-dimensional parameter space shown in **Fig. 5e**, they span an iso-velocity surface (blue points in **Fig. 5e**) at vanishing velocity, in other words, their pattern interfaces are stabilized with little or no moving. To illustrate the local orientation of the surface, we selected 9,261 points (enumerated on a 3D grid Y∈ [0.034,0.044] in steps ΔY = 0.0005, $k_1 \in [1.05,2.05]$ in steps $\Delta k_1 = 0.05$, and $q_2 \in [0.045,0.055]$ in steps $\Delta q_2 = 0.0005$) in the neighborhood of a benchmark point $\Omega^*(\gamma^* = 0.039, k_1^* = 1.55, q_2^* = 0.05)$, as shown by the brown box in **Fig. 6a**, top. The least-square fit of computed interface velocity to a linear function yields:

$$f(\gamma, k_1, q_2) = -0.0308 \times (\gamma - \gamma^*) - 6.08 \times 10^{-4} \times (k_1 - k_1^*) + 0.02 \times (q_2 - q_2^*), \quad (9)$$

with the coefficient of determination:

$$R^2 = 1 - \frac{\sum_{i=1}^{9261}[v_{\mathrm{I}}(\Omega_i) - f(\Omega_i)]^2}{\sum_{i=1}^{9261}\left[v_{\mathrm{I}}(\Omega_i) - \frac{1}{9261}\sum_{j=1}^{9261} v_{\mathrm{I}}(\Omega_i)\right]^2} = 0.9918. \quad (10)$$

The coefficients in **Eq. (9)** give the ascending gradient of the interface velocity (**Fig. 6a**, bottom).

Within the assumed relationships adopted for parameter reduction (see **Sec. 2.1**), **Eq. (9)** shows a strong dependence of the interface velocity on basal on/off-rates Y and activation intensity q_2, but weak sensitivity to responsive concentration k_1 in the inspected parameter region. Interestingly, increase in the basal on/off-rates Y and the self-activation rate q_2 have opposite effects on the interface velocity, which can be attributed to the asymmetric 5-node network topology. In a more realistic scenario, one may consider on/off-rates for different molecular species and their pairwise interactions separately and explore the relationships in a much larger parameter space. A formula similar to **Eq. (9)**, using a linear expansion around the parameter sets balanced for a zero-velocity interface, enables quantitative prediction of the interface velocity against individual or simultaneous changes of parameters, even when knowledge of the polarity circuit is incomplete. In particular, the parameter-dependent interface velocity picture potentially enables biologists to manipulate and even synthesize the cell polarization pattern by rational modulation of parameters, controlling the interface location for specific physiological functions, such as designating a desired cell volume partition ratio [Hubatsch et al., *Nat. Phys.*, 2019; Guan et al., *Phys. Rev. E*, 2021].

Experimental studies have revealed that the interface localization in the *C. elegans* zygotic cell polarization pattern provides an accurate spatial cue to regulate the dynamics of their downstream molecules, like the protein LIN-5 and microtubules that control cell division and volume partition [Schneider et al., *Annu. Rev. Genet.*, 2003; Ajduk et al., *Mol. Hum. Reprod.*, 2016], while the acquired cell volume has been reported to have a chain effect in its cell cycle, cell position, and other behaviors [Fickentscher et al., *New J. Phys.*, 2018; Guan et al., *Phys. Rev. E*, 2021; Fickentscher et al., *Phys. Rev. Lett.*, 2016; Tian et al., *Phys. Biol.*, 2020]. As in the 2-node network, the precise control of the stable position of the interface can be realized by taking the parameters corresponding to the opposite direction of the interface velocity on both sides of the interface. Based on the parameter set Ω* which gives out the most stable pattern (**Fig. 6b** and Movie S5), two modifications are adopted to generate patterns with opposite interface velocity:

1. Increasing the activation intensity between [A] and [C] (q_{C2}^{A} & q_{A2}^{C}) to 0.12 leads to the interface traveling backward, and [A] and [C] finally dominate the whole domain of the membrane.

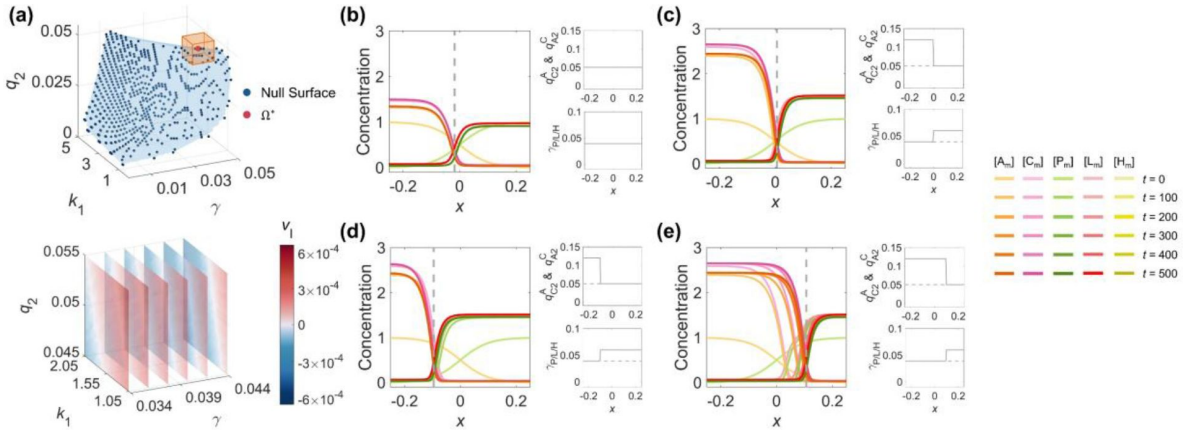

Fig. 6.

The control of the interface velocity and position by adjusting parameters in a multi-dimensional system.

(a) The parameter space (1st row) and the linear relationship (2nd row) between interface velocity and parameters. The discrete viable parameter space of WT network is fitted by a blue curved surface to represent its null surface with little or no pattern interface moving (1st row). The benchmark point $\Omega^*(\gamma^* = 0.039, k_1^* = 1.55, q_2^* = 0.05)$ and its neighborhood are marked by an orange cube. Centering on the benchmark point Ω*, the relationship between the velocity interface and parameters in the region marked by the orange cube is shown by slice planes orthogonal to the Y-axis at the values 0.034, 0.036, 0.038, 0.04, 0.042, and 0.044 (2nd row). The darker the red is, the faster the interface is moving toward the posterior pole; the darker the blue is, the faster the interface is moving toward the anterior pole; the closer the color is to white, the more stable the interface is. (b-d) As in **Fig. 4**, the control of the interface position by spatially inhomogeneous parameters corresponding to opposite interface velocities on two sides of the interface can be applied to the *C. elegans* 5-node network. (b) Using Ω* as a representative, spatially uniform parameters (2nd column) generate a stable polarity pattern (1st column). (c) On top of (b), a stable polarity pattern (1st column) with its interface around $x = 0$ can be obtained by increasing q_{C2}^{A} & q_{A2}^{C} to 0.12 at $x < 0$ and increasing Y_P, Y_L, and Y_H to 0.06 at $x > 0$ (2nd column). (d) As in (c) but changing the step position to $x = -0.1$ (2nd column), the interface stabilizes around $x = -0.1$ (1st column). (e) As in (c), but changing the step position to $x = 0.1$ (2nd column), the interface stabilizes around $x = 0.1$ (1st column). For each parameter set, the corresponding spatial concentration distribution of $[A_m]$, $[C_m]$, $[P_m]$, $[L_m]$, and $[H_m]$ at $t = 0$, 100, 200, 300, 400, and 500 are shown beneath with a color scheme listed on the right. Note that all the interface positions in (b-e) are marked by the vertical dashed line in gray.

2. Increasing the basal on-rate of posterior proteins (Y_P, Y_L, Y_H) to 0.06 results in the interface traveling forward, and [P], [L] and [H] finally dominate the whole domain of the membrane.

Combining the two sets of parameters with its step switch located at $x = 0$ ((i) on the left and (ii) on the right), the stabilized polarity interface settles around $x = 0$ (**Fig. 6c** and Movie S5). The interface position turns tunable as the step switch moves to $x = -0.1$ (**Fig. 6d** and Movie S5) and $x = 0.1$ (**Fig. 6e** and Movie S5). One pre-known example in reality that matches this scheme is the asymmetric division of the P2 and P3 cells (the granddaughter and great-granddaughter cells of the *C. elegans* zygote P0), where the extracellular protein MES-1 and intracellular protein SRC-1 transduct signals from the EMS and E cells (the sister cell of P2 and its posterior daughter cell), inducing polarity reversal by affecting the on-rate of PAR-2 [Arata et al., *Development*, 2010; Seirin-Lee, *J. Theor. Biol.*, 2016]. Such a scheme depicts the introduction of extracellular or intracellular cues that break the spatial uniformity of parameters and tune the stable localization of interface, serving as a theoretical basis for controlling oriented cell division with designated volume partition and fate differentiation [Arata et al., *Development*, 2010; Hubatsch et al., *Nat. Phys.*, 2019; Schubert et al., *Mol. Cell*, 2000].

3. Discussion and conclusion

Cell polarization is a fundamental issue in both prokaryotes and eukaryotes, playing crucial roles in diverse biological phenomena ranging from chemotaxis to embryogenesis [Nance, *J. Cell Biol.*, 2014; Kondo et al., *J. Leukoc. Biol.*, 2019]. The reaction-diffusion network responsible for cell polarization has been a long-term research focus for both experimentalists and theorists, who have identified many interactive functional molecules, discovered underlying design principles for networks, and even synthesized new systems *de novo* [Koorman et al., *Nat. Cell Biol.*, 2016; Lang et al., *Development*, 2017; Tostevin et al., *Biophys J*, 2008; Chau et al., *Cell*, 2012; Lin et al., *Nat. Commun.*, 2021; Watson et al., *Cell*, 2023]. In this paper, we focus on a basic problem – how to control the cell polarization pattern stability over time and regulate the stabilized interface localization, from the perspective of a reaction-diffusion network. First, we established a computational pipeline to search the viable parameter sets in an *N*-node (molecular species) network that can achieve a stable cell polarization pattern. The simple antagonistic network with only two nodes was revealed to be unstable (*i.e.*, transit from a polarized distribution to a homogeneous distribution spontaneously) when any of the 3 unbalanced modifications (*i.e.*, single-sided self-regulation, single-sided additional regulation, and unequal system parameters) were introduced. To recover stable polarization, two strategies are proposed: (i) the combination of two unbalanced modifications with opposite effects; (ii) the spatially inhomogeneous parameter values, either of which can lead to opposite interface velocity. Additionally, the stable interface localization can be discretionarily regulated by the step-like parameter profile and contributes to the asymmetric geometry of the cell polarization pattern, potentially providing a spatial cue for significant physiological functions like unequal cell volume partition and consequent punctuated cell movement [Fickentscher et al. *New J. Phys.*, 2018; Guan et al., *Phys. Rev. E*, 2021; Fickentscher et al., *Phys. Rev. Lett.*, 2016; Tian et al., *Phys. Biol.*, 2020]. Analogous conclusions are further identified in the *C. elegans* network summarized experimentally which obtains larger parameter space and is higher robustness against parameter perturbations, supporting them as strategies indeed applied in real biological scenarios. Importantly, the linear relationship between the interface velocity and biophysical parameters serves as a useful tool to characterize and predict how the cell polarization pattern, especially where the interface is located or moved toward, responds to parameter changes; this not only helps understand the regulatory molecular species and pathways, as well as the biophysical parameters learned from experiments, play their role but also guides the design of artificial cell polarization system with desired functions. The joint study on a simple 2-node network and *C. elegans* 5-node network demonstrated that the cell

polarization pattern with both stability and asymmetry can be explicitly realized by a combinatorial network and spatially inhomogeneous parameters, which is expected to facilitate the interpretation of natural systems and design of artificial systems.

Although we deciphered the stability and asymmetry of the pattern generated by the *C. elegans* cell polarization network, additional experimental details are required to achieve a more comprehensive understanding of this system, as outlined below.

1. Although the model in this paper has tried to incorporate as many molecular species as possible for the maintenance phase of cell polarization, the actual network may include yet unidentified molecular species. This also extends to interactions, as well as their intensity, between molecular species. For instance, the components of the molecular complex (*e.g.*, PAR-3/PAR-6/PKC-3), often treated as a single entity in theoretical studies [Tostevin et al., *Biophys. J.*, 2008; Gross et al., *Nat. Phys.*, 2019; Seirin-Lee et al., *Cells*, 2020; Lim et al., *Cell Rep.*, 2021], might not be ideally identical concerning their slightly different polarized patterns [Wang et al., *Nat. Cell Biol.*, 2017]. The PAR-6 and PKC-3 also bind CDC-42, in addition to PAR-3, to mediate membrane association of CHIN-1 via phosphorylation, and such joint effect was previously described to be governed by a single node, CDC-42 [Lim et al., *Cell Rep.*, 2021]. Future experimental validation is needed to detail whether and how the molecular species described in Table S2 (and beyond) interact with each other.
2. The large number of molecular species introduces substantial parameter complexity, with myriad possible value assignments. Simplifying the model is necessary to manage computational costs unless all parameters can be measured accurately *in vivo* [Wang et al., *Nat. Commun.*, 2020].
3. Quantitative biological details, such as the concentration distributions, diffusions, productions, and degradations of molecular species on the cell membrane versus in the cell cytosol [Tostevin et al., *Biophys. J.*, 2008; Goehring et al., *Science*, 2011; Kravtsova et al., *Bull. Math. Biol.*, 2014; Sailer et al., *Dev. Cell*, 2015; Seirin-Lee, et al., *J. Theor. Biol.*, 2015; Seirin-Lee et al., *J. Theor. Biol.*, 2016; Gross et al., *Nat. Phys.*, 2019; Seirin-Lee et al., *J. Math. Biol.*, 2020; Lim et al., *Cell Rep.*, 2021] and the precise mathematical forms of regulatory interactions (*e.g.*, Hill equations or product equations) [Goehring et al., *Science*, 2011; Seirin-Lee et al., *Cells*, 2020; Lim et al., *Cell Rep.*, 2021], challenge model assumptions and hinder the unification of parameter value with unit between theory and experiment [Tostevin et al., *Biophys. J.*, 2008; Kravtsova et al., *Bull. Math. Biol.*, 2014]. Nonetheless, prior studies integrating theory and experiments have demonstrated that unveiling mathematical principles for regulatory networks does not strictly depend on unit unification; numerical network structure and parameter analysis can still effectively draw the mathematical principles for guiding the synthesis of artificial networks in reality, including the one for cell polarization [Elowitz et al., *Nature*, 2000; Gardner et al., *Nature*, 2000; Ma et al., *Cell*, 2009; Chau et al., *Cell*, 2012].
4. Incorporating biological processes across temporal stages and spatial scales could offer a more holistic understanding of cell polarization. On one hand, early stages, such as sperm entry and the establishment phase, which involve active actomyosin contractility and flow drive PAR-3/PAR-6/PKC-3 to be localized in the anterior, can provide insights into how initial polarized concentration distributions are achieved [Cuenca et al., *Development*, 2003; Motegi et al., *Nat. Cell Biol.*, 2011]. On the other hand, molecular (e.g., downstream localization of the myosin motor NMY-2 to the anterior cortex mediated by CDC-42 and PAR-2 [Goehring et al., *J. Cell Biol.*, 2011; Rose et al., *WormBook*, 2014; Geβele et al., *Nat. Commun.*, 2020]) and cellular (asymmetric segregation of cell volume and molecular content, mediated by molecular species like MES-1 and SRC-1 [Arata et al., *Development*, 2010; Seirin-Lee, *J. Theor. Biol.*, 2016]) effect of cell polarization can further elucidate its various roles in embryogenesis.

Beyond the *C. elegans* zygote studied in this paper, cell polarization also exists in later stages of *C. elegans* embryogenesis as well as in other organisms, where diverse functional dynamics have been reported [Rose et al., *WormBook*, 2014; Knoblich et al., *Nat. Rev. Mol. Cell Biol.*, 2001]. Governed by the cell polarization, the *C. elegans* embryo actually proceeds 4 rounds of asymmetric division to produce 4 somatic founder cells, then such reaction-diffusion pattern will lose its sharp transition plane as it is unscalable over cell size, leading to symmetric cell division at last [Hubatsch et al., *Nat. Phys.*, 2019]. Furthermore, as the reaction-diffusion network itself is not particularly constricted in the cellular scale, but also possibly in subcellular and multicellular scales, it would be interesting to investigate if the general principles proposed in this paper are also at work for the network programming and pattern modulation in other scales [Chao et al., *Cell*, 2014; Guan et al., *Sci. Adv.*, 2022].

Nowadays, the *de novo* construction of artificial cells with designated new functions is emerging, demanding theoretical guidance about how to synthesize the molecular control circuits beneath [Zhou et al., *Science*, 2023; Zhu et al., *Sci. Adv.*, 2023]. Like toggle switch, oscillation, and adaptation [Gardner et al., *Nature*, 2000; Zhou et al., *Science*, 2023; Sun et al., *Nucleic Acids Res.*, 2022], the polarized distribution of molecular species (accounting for cell polarization) is also another elementary behavior in a cell, and the corresponding circuits have been synthesized successfully around a decade ago [Chau et al., *Cell*, 2012]. However, it remains unclear whether the distribution pattern (*e.g.*, the transition plane of a molecular species) can be altered while maintaining stability. Taking the *C. elegans* network as an example, our computational framework has been demonstrated to be capable of deciphering such a real reaction-diffusion network with pattern stability and asymmetry, and has been packed as a user-friendly software, *PolarSim* (Supplemental Text); thus we believe it can be used for not only understanding the natural molecular networks reported before but also designing new molecular networks in the polarized cells with more physiological functions, for example, with tunable transition plane of molecular species to guide the allocation of downstream fate determinants and unequal cleavage during cytokinesis [Fickentscher et al., *Sci. Rep.*, 2017]. In the future, our computational framework for cell polarization network could be linked to the one about cytoskeleton activity, achieving a more comprehensive modeling description for cell division [Pavin et al., *New J. Phys.*, 2012; Ma et al., *New J. Phys.*, 2014].

Acknowledgements

We thank Prof. Wei Wang, Dr. Daimin Li, Peng Xie, Shiyu Shen, and Qi Ding for their assistance in the numerical simulation, and Prof. Hongli Wang for his constructive advice on the project. We are grateful to Dr. Siyu Li, Dr. Baoshuang Shang, Dr. Shipu Xu, and Yuqing Zhong for their help during Yixuan Chen and Guoye Guan's academic visit to Songshan Lake Materials Laboratory. We appreciate Zhengyang Han for his assistance in improving the paper materials. Gratitude is extended to Prof. Zhongying Zhao for his help during Guoye Guan's academic visit to Hong Kong Baptist University. This work was supported by funding from the National Natural Science Foundation of China (12090053 and 32088101) and the Research Grants Council of the Hong Kong SAR (12303219). Computation was performed partly on the High-Performance Computing Platform at Peking University.

Additional information

Author contributions

Y.C. and G.G. designed and conceived the project, and wrote the paper; Y.C., G.G., L.- H.T., and C.T. performed research and conducted analysis; L.-H.T. and C.T. supervised the project and revised the paper.

Additional files

Supplementary material.

Table S1. *The parameter description of the reaction-diffusion model for simulating a cell polarization network.*

Table S2. *The literature summary on the cell polarization network in the C. elegans zygote.*

Movie S1. *The concentration distribution of each molecular species on the cell membrane over time generated by the antagonistic 2-node network and the ones with a single modification added, corresponding to Fig. 1*

Movie S2. *The concentration distribution of each molecular species on the cell membrane over time generated by the antagonistic 2-node network and the ones with a single modification or two combinatorial modifications added, corresponding to Fig. 2.*

Movie S3. *The concentration distribution of each molecular species on the cell membrane over time generated by the antagonistic 2-node network with spatially inhomogeneous parameters, corresponding to Fig. 4.*

Movie S4. *The concentration distribution of each molecular species on the cell membrane over time generated by the 4-Node, LGL-1-, and WT networks, corresponding to Fig. 5b-d.*

Movie S5. *The concentration distribution of each molecular species on the cell membrane over time generated by the C. elegans 5-node network with spatially inhomogeneous parameters, corresponding to Fig. 6b-e.*

References

[1] Aceto D, Beers M, Kemphues KJ (2006) **Interaction of PAR-6 with CDC-42 is required for maintenance but not establishment of PAR asymmetry in C. elegans** *Dev Biol* **299**:386–97

[2] Ajduk A, Zernicka-Goetz M (2016) **Polarity and cell division orientation in the cleavage embryo: from worm to human** *Mol Hum Reprod* **22**:691–703

[3] Arata Y, Lee JY, Boldstein B, et al. (2010) **Extracellular control of PAR protein localization during asymmetric cell division in the C. elegans embryo** *Development* **137**:3337–45

[4] Beatty A, Morton D, Kemphues K (2010) **The C. elegans homolog of Drosophila lethal giant larvae functions redundantly with PAR-2 to maintain polarity in the early embryo** *Development* **137**:3995–4004

[5] Beatty A, Morton DG, Kemphues K (2013) **PAR-2, LGL-1 and the CDC-42 GAP CHIN-1 act in distinct pathways to maintain polarity in the C. elegans embryo** *Development* **140**:2005–14

[6] Bilder D, Li M, Perrimon N (2000) **Cooperative regulation of cell polarity and growth by Drosophila tumor suppressors** *Science* **289**:113–6

[7] Blanchoud S, Busso C, Naef F, et al. (2015) **Quantitative analysis and modeling probe polarity establishment in C. elegans embryos** *Biophys J* **108**:799–809

[8] Chao JT, Wong AKO, Tavassoli S, et al. (2014) **Polarization of the endoplasmic reticulum by ER-septin tethering** *Cell* **158**:620–32

[9] Chau AH, Walter JM, Gerardin J, et al. (2012) **Designing synthetic regulatory networks capable of self-organizing cell polarization** *Cell* **151**:320–32

[10] Cuenca AA, Schetter A, Aceto D, et al. (2003) **Polarization of the C. elegans zygote proceeds via distinct establishment and maintenance phases** *Development* **130**:1255–65

[11] Doe CQ, Bowerman B (2001) **Asymmetric cell division: fly neuroblast meets worm zygote** *Curr Opin Cell Biol* **13**:68–75

[12] Elowitz MB, Leibler S (2000) **A synthetic oscillatory network of transcriptional regulators** *Nature* **403**:335–8

[13] Etienne-Manneville S, Hall A (2002) **Rho GTPases in cell biology** *Nature* **420**:629–35

[14] Fickentscher R, Krauss SW, Weiss M (2018) **Anti-correlation of cell volumes and cell-cycle times during the embryogenesis of a simple model organism** *New J Phys* **20**:113001

[15] Fickentscher R, Weiss M (2017) **Physical determinants of asymmetric cell divisions in the early development of Caenorhabditis elegans** *Sci Rep* **7**:9369

[16] Fickentscher R, Struntz P, Weiss M (2016) **Setting the clock for fail-safe early embryogenesis** *Phys Rev Lett* **117**:188101

[17] Fishman GS (1995) **Monte Carlo: Concepts, algorithms, and applications** New York, NY: Springer

[18] Gardner TS, Cantor CR, Collins JJ (2000) **Construction of a genetic toggle switch in Escherichia coli** *Nature* **403**:339–42

[19] Geßele R, Halatek J, Würthner L, et al. (2020) **Geometric cues stabilise long-axis polarisation of PAR protein patterns in C. elegans** *Nat Commun* **11**:539

[20] Goehring NW, Hoege C, Grill SW, et al. (2011) **PAR proteins diffuse freely across the anterior-posterior boundary in polarized C. elegans embryos** *J Cell Biol* **193**:583–94

[21] Goehring NW, Trong PK, Bois JS, et al. (2011) **Polarization of PAR proteins by advective triggering of a pattern-forming system** *Science* **334**:1137–41

[22] Goldstein B, Hird SN (1996) **Specification of the anteroposterior axis in Caenorhabditis elegans** *Development* **122**:1467–74

[23] Goodrich LV, Strutt D (2011) **Principles of planar polarity in animal development** *Development* **138**:1877–92

[24] Gotta M, Abraham MC, Ahringer J (2001) **CDC-42 controls early cell polarity and spindle orientation in C. elegans** *Curr Biol* **11**:482–8

[25] Gross P, Kumar KV, Goehring NW, et al. (2019) **Guiding self-organized pattern formation in cell polarity establishment** *Nat Phys* **15**:293–300

[26] Guan C, Qiao L, Xiong Y, et al. (2022) **Coactivation of antagonistic genes stabilizes polarity patterning during shoot organogenesis** *Sci Adv* **8**:eabn0368

[27] Guan G, Wong MK, Zhao Z, et al. (2021) **Volume segregation programming in a nematode's early embryogenesis** *Phys Rev E* **104**:054409

[28] Hoege C, Constantinescu A, Schwager A, et al. (2010) **LGL can partition the cortex of one-cell Caenorhabditis elegans embryos into two domains** *Curr Biol* **20**:1296–303

[29] Hubatsch L, Peglion F, Reich JD, et al. (2019) **A cell-size threshold limits cell polarity and asymmetric division potential** *Nat Phys* **15**:1075–85

[30] Jankele R, Jelier R, Gönczy P (2021) **Physically asymmetric division of the C. elegans zygote ensures invariably successful embryogenesis** *eLife* **10**:e61714

[31] Kemphues KJ, Priess JR, Morton DG, et al. (1988) **Identification of genes required for cytoplasmic localization in early C. elegans embryos** *Cell* **52**:311–20

[32] Kim M, Datta A, Brakeman P, et al. (2007) **Polarity proteins PAR6 and aPKC regulate cell death through GSK-3β in 3D epithelial morphogenesis** *J Cell Sci* **120**:2309–17

[33] Knoblich JA (2001) **Asymmetric cell division during animal development** *Nat Rev Mol Cell Biol* **2**:11–20

[34] Kondo Y, Ledderose C, Slubowski CJ, et al. (2019) **Frontline Science: Escherichia coli use LPS as decoy to impair neutrophil chemotaxis and defeat antimicrobial host defense** *J Leukoc Biol* **106**:1211–9

[35] Koorman T, Klompstra D, van der Voet M, et al. (2016) **A combined binary interaction and phenotypic map of C. elegans cell polarity proteins** *Nat Cell Biol* **18**:337–46

[36] Kravtsova N, Dawes AT (2014) **Actomyosin regulation and symmetry breaking in a model of polarization in the early Caenorhabditis elegans embryo** *Bull Math Biol* **76**:2426–48

[37] Kumfer KT, Cook SJ, Squirrell JM, et al. (2010) **CGEF-1 and CHIN-1 regulate CDC-42 activity during asymmetric division in the Caenorhabditis elegans embryo** *Mol Biol Cell* **21**:266–77

[38] Lang CF, Munro E (2017) **The PAR proteins: from molecular circuits to dynamic self-stabilizing cell polarity** *Development* **144**:3405–16

[39] Lin DW, Liu Y, Lee YQ, et al. (2021) **Construction of intracellular asymmetry and asymmetric division in Escherichia coli** *Nat Commun* **12**:888

[40] Lim YW, We FL, Shankar P, et al. (2021) **A balance between antagonizing PAR proteins specifies the pattern of asymmetric and symmetric divisions in C. elegans embryogenesis** *Cell Rep* **36**:109326

[41] Ma R, Laan L, Dogterom M, et al. (2014) **General theory for the mechanics of confined microtubule asters** *New J Phys* **16**:013018

[42] Ma W, Trusina A, El-Samad H, et al. (2009) **Defining network topologies that can achieve biochemical adaptation** *Cell* **138**:760–73

[43] Macara IG (2004) **Parsing the polarity code** *Nat Rev Mol Cell Biol* **5**:220–31

[44] The MathWorks Inc (2022) **MATLAB version: 9.13.0 (R2022b)** Natick, Massachusetts: The MathWorks Inc

[45] Morita Y, Seirin-Lee S (2021) **Long time behavior and stable patterns in high-dimensional polarity models of asymmetric cell division** *J Math Biol* **82**:66

[46] Motegi F, Zonies S, Hao Y, et al. (2011) **Microtubules induce self-organization of polarized PAR domains in Caenorhabditis elegans zygotes** *Nat Cell Biol* **13**:1361–7

[47] Munro E, Nance J (2004) **Cortical flows powered by asymmetrical contraction transport PAR proteins to establish and maintain anterior-posterior polarity in the early C. elegans embryo** *Dev Cell* **7**:413–24

[48] Nance J (2014) **Getting to know your neighbor: cell polarization in early embryos** *J Cell Biol* **206**:823–32

[49] Pavin N, Laan L, Ma R, et al. (2012) **Positioning of microtubule organizing centers by cortical pushing and pulling forces** *New J Phys* **14**:105025

[50] Rose LS, Gönczy P (2014) **Polarity establishment, asymmetric division and segregation of fate determinants in early C. elegans embryo** *WormBook* :1–43

[51] Sailer A, Anneken A, Li Y, et al. (2015) **Dynamic opposition of clustered proteins stabilizes cortical polarity in the C. elegans zygote** *Dev Cell* **35**:131–42

[52] Schneider SQ, Bowerman B (2003) **Cell polarity and the cytoskeleton in the Caenorhabditis elegans zygote** *Annu Rev Genet* **37**:221–49

[53] Schubert CM, Lin R, de Vries CJ, et al. (2000) **MEX-5 and MEX-6 function to establish soma/germline asymmetry in early C. elegans embryos** *Mol. Cell* **5**:671–82

[54] Seirin-Lee S (2020) **Asymmetric cell division form a cell to cells: shape, length, and location of polarity domain** *Dev Growth Differ* **62**:188–95

[55] Seirin-Lee S (2016) **Positioning of polarity formation by extracellular signaling during asymmetric cell division** *J Theor Biol* **400**:52–64

[56] Seirin-Lee S, Shibata T (2015) **Self-organization and advective transport in the cell polarity formation for asymmetric cell division** *J Theor Biol* **382**:1–14

[57] Seirin-Lee S, Gaffney EA, Dawes AT (2020) **CDC-42 interactions with Par proteins are critical for proper patterning in polarization** *Cells* **9**:2036

[58] Seirin-Lee S (2021) **The role of cytoplasmic MEX-5/6 polarity in asymmetric cell division** *Bull Math Biol* **83**:29

[59] Seirin-Lee S, Sukekawa T, Nakahara T, et al. (2020) **Transitions to slow or fast diffusions provide a general property for in-phase or anti-phase polarity in a cell** *J Math Biol* **80**:1885–917

[60] Sulston JE, Schierenberg E, White JG, et al. (1983) **The embryonic cell lineage of the nematode Caenorhabditis elegans** *Dev Biol* **100**:64–119

[61] Sun Z, Wei W, Zhang M, et al. (2022) **Synthetic robust perfect adaptation achieved by negative feedback coupling with linear weak positive feedback** *Nucleic Acids Res* **50**:2377–86

[62] Tian B, Guan G, Tang L-H, et al. (2020) **Why and how the nematode's early embryogenesis can be precise and robust: a mechanical perspective** *Phys Biol* **17**:026001

[63] Tostevin F, Howard M (2008) **Modeling the establishment of PAR protein polarity in the one-cell C. elegans embryo** *Biophys J* **95**:4512–22

[64] Wang JT, Seydoux G (2013) **Germ cell specification** *Adv Exp Med Biol* **757**:17–39

[65] Wang S-C, Low TYF, Nishimura Y, et al. (2017) **Cortical forces and CDC-42 control clustering of PAR proteins for Caenorhabditis elegans embryonic polarization** *Nat Cell Biol* **19**:988–95

[66] Wang T, You L (2020) **The persistence potential of transferable plasmids** *Nat Commun* **11**:5589

[67] Watson JL, Krüger LK, Ben-Sasson AJ, et al. (2023) **Synthetic Par polarity induces cytoskeleton asymmetry in unpolarized mammalian cells** *Cell* **186**:4710–27

[68] Zhou Z, Liu Y, Feng Y, et al. (2023) **Engineering longevity—design of a synthetic gene oscillator to slow cellular aging** *Science* **380**:3760381

[69] Zhu R, Santat LA, Markson JS, et al. (2023) **Reconstitution of morphogen shuttling circuits** *Sci Adv* **9**:eadf9336

Author information

Yixuan Chen[†]

South Bay Interdisciplinary Science Center, Songshan Lake Materials Laboratory, Guangdong, China, Department of Physics, Sichuan University, Sichuan, China, School of Physics, Peking University, Beijing, China

[†]These authors contributed equally to this work.

Guoye Guan[†a.b.]

South Bay Interdisciplinary Science Center, Songshan Lake Materials Laboratory, Guangdong, China, Center for Quantitative Biology, Peking University, Beijing, China, Department of Physics, Hong Kong Baptist University, Hong Kong, China

[†]These authors contributed equally to this work.

[a.]Department of Systems Biology, Harvard Medical School, Boston, United States

[b.]Department of Data Science, Dana-Farber Cancer Institute, Boston, United States

Lei-Han Tang

South Bay Interdisciplinary Science Center, Songshan Lake Materials Laboratory, Guangdong, China, Department of Physics, Hong Kong Baptist University, Hong Kong, China, Institute of Computational and Theoretical Studies, Hong Kong Baptist University, Hong Kong, China, State Key Laboratory of Environmental and Biological Analysis, Hong Kong Baptist University, Hong Kong, China

For correspondence: lhtang@hkbu.edu.hk

Chao Tang

School of Physics, Peking University, Beijing, China, Center for Quantitative Biology, Peking University, Beijing, China, Peking-Tsinghua Center for Life Sciences, Peking University, Beijing, China

For correspondence: tangc@pku.edu.cn

Editors

Reviewing Editor

Mariana Gómez-Schiavon

Universidad Nacional Autónoma de México, Querétaro, Mexico

Senior Editor

Aleksandra Walczak

CNRS, Paris, France

Joint Public Review:

In this manuscript, the authors aim to evaluate the robustness of stable asymmetric polarization patterns by analyzing both a minimal 2-node network and a more biologically

realistic 5-node network based on the C. elegans polarization system. They introduce a computational pipeline for systematically exploring reaction-diffusion network dynamics. Their study highlights the limitations of the widely used 2-node antagonistic network, demonstrating its susceptibility to simple modifications that disrupt polarization. However, they show that polarization stability can be restored by combining multiple regulatory mechanisms, and that spatially varying kinetic parameters can fine-tune the interface position. The authors further investigate the 5-node network of C. elegans, identifying key parameters that enhance its robustness against perturbations. Their findings provide novel insights into the mechanisms that ensure stable polarization in biological systems.

The major strengths of this work lie in its rigorous computational approach and the clarity of its findings. The authors demonstrate that the widely used 2-node antagonistic network is highly sensitive to parameter changes, requiring precise fine-tuning to maintain stable polarization. However, they show that stability can be restored through compensatory modifications, which expand the range of parameter sets supporting polarization. By further exploring spatial parameter variations, the authors reveal how compensatory adjustments can stabilize polarization patterns, offering insights into potential biological mechanisms regulating interface localization.

Extending their analysis to the C. elegans polarization network, the authors construct a 5-node model grounded in an extensive literature review. Their computational pipeline identifies key parameters that enhance robustness, and their model successfully replicates experimental observations, even in mutant conditions. Notably, among 34 possible network structures, only the naturally evolved 5-node network with mutual inhibition between specific components maintains stable polarization, highlighting its evolutionary optimization. This work significantly advances our understanding of polarization maintenance and provides a valuable framework for future in silico experiments.

Despite its strengths, the study has some limitations related to simplifying assumptions. The model neglects cortical flows and the role of actomyosin dynamics, which are known to be crucial during the establishment phase of polarization in the C. elegans zygote. While the authors focus on the maintenance phase, the absence of these biomechanical effects may limit the model's applicability to the full polarization process. Additionally, the assumption of infinitely fast cytoplasmic diffusion disregards potential effects of cytoplasmic flows on the stability of molecular distributions. Experimental measurements suggest that cytoplasmic diffusion coefficients are only an order of magnitude higher than membrane diffusion coefficients, meaning that finite diffusion combined with cytoplasmic flows could influence polarization stability. Although the authors acknowledge and discuss these limitations, incorporating these effects in future models could provide a more complete picture of the polarization dynamics in C. elegans embryos.

https://doi.org/10.7554/eLife.96421.2.sa1

Author response:

The following is the authors' response to the original reviews

> ***eLife Assessment***
>
> *This manuscript makes valuable contributions to our understanding of cell polarisation dynamics and its underlying mechanisms. Through the development of a computational pipeline, the authors provide solid evidence that compensatory actions, whether regulatory or spatial, are essential for the robustness of the polarisation pattern. However, a more comprehensive validation against experimental data and a proper*

> *estimation of model parameters are required for further characterization and predictions in natural systems, such as the C. elegans embryo.*

We sincerely thank the editor(s) for their pertinent assessment. We have carefully considered the constructive recommendations and made the necessary revisions in the manuscript, which are also detailed in this response letter. We have implemented most of the revisions requested by the reviewers. For the few requests we did not fully accept, we have provided justifications. The corresponding revisions in both the Manuscript and Supplementary Information are highlighted with a yellow background. To provide a more comprehensive validation against experimental data and model parameters used for characterizing and predicting natural systems, we reproduced the qualitative and semi-quantitative phenomenon in three more experimental groups previously published (Section 2.5; Fig. S8) [Gotta et al., Curr. Biol., 2001; Aceto et al., Dev. Biol., 2006]. Combined with the original experiments (Section 2.5; Fig. S7) [Hoege et al., Curr. Biol., 2010; Beatty et al., Development, 2010; Beatty et al., Development, 2013], now we have reproduced five experimental groups in total (two acting on LGL-1 and three on CDC-42), comprising eight perturbed conditions and using wild-type as the reference. These results effectively demonstrate how comprehensively the network structure and parameters capture the characteristics of the *C. elegans* embryo. We have also acknowledged the limitations of the current cell polarization model and provided, in 2. Results and 3. Discussion and conclusion, a detailed outline of potential model improvements.

> ***Joint Public Review:***
>
> *The polarisation phenomenon describes how proteins within a signalling network segregate into different spatial domains. This phenomenon holds fundamental importance in biology, contributing to various cellular processes such as cell migration, cell division, and symmetry breaking in embryonic morphogenesis. In this manuscript, the authors assess the robustness of stable asymmetric patterns using both a previously proposed minimal model of a 2-node network and a more realistic 5-node network based on the C. elegans cell polarisation network, which exhibits anterior-posterior asymmetry. They introduce a computational pipeline for numerically exploring the dynamics of a given reaction-diffusion network and evaluate the stability of a polarisation pattern. Typically, the establishment of polarisation requires the mutual inhibition of two groups of proteins, forming a 2-node antagonistic network. Through a reaction-diffusion formulation, the authors initially demonstrate that the widely-used 2-node antagonistic network for creating polarised patterns fails to maintain the polarised pattern in the face of simple modifications. However, the collapsed polarisation can be restored by combining two or more opposing regulations. The position of the interface can be adjusted with spatially varied kinetic parameters. Furthermore, the authors show that the 5-node network utilised by C. elegans is the most stable for maintaining polarisation against parameter changes, identifying key parameters that impact the position of the interface.*

We sincerely thank the editor(s) for the pertinent summary!

> *While the results offer novel and insightful perspectives on the network's robustness for cell polarisation, the manuscript lacks comprehensive validation against experimental data, justified node-node network interactions, and proper estimation of model parameters (based on quantitative measurements or molecular intensity distributions). These limitations significantly restrict the utility of the model in making meaningful predictions or advancing our understanding of cell polarisation and pattern formation in natural systems, such as the C. elegans embryo.*

We sincerely thank the editor(s) for the comment!

To provide a more comprehensive validation against experimental data and model parameters, we reproduced the qualitative and semi-quantitative phenomenon in three more experimental groups previously published (Section 2.5; Fig. S8) [Gotta et al., Curr. Biol., 2001; Aceto et al., Dev. Biol., 2006]. Combined with the original experiments (Section 2.5; Fig. S7) [Hoege et al., Curr. Biol., 2010; Beatty et al., Development, 2010; Beatty et al., Development, 2013], now we have reproduced five experimental groups in total (two acting on LGL-1 and three on CDC-42), comprising eight perturbed conditions and using wild-type as the reference. These meaningful predictions effectively demonstrate the utility of our model's network structure and parameters in advancing our understanding of cell polarisation and pattern formation in natural systems, exemplified by the *C. elegans* embryo.

We have also acknowledged the limitations of the current cell polarization model and provided, in 2. Results and 3. Discussion and conclusion, a detailed outline of potential model improvements. The limitations include, but are not limited to, issues involving "node-node network interactions" and the "proper estimation of model parameters (based on quantitative measurements or molecular intensity distributions)", both of which rely on experimental measurements of biological information. However, comprehensive experimental measurement data on every molecular species, their interactions, and each species' intensity distribution in space and time were not fully available from prior research. Refinement is lacking for some of these interactions, potentially requiring years of additional experimentation. Moreover, for certain species at specific developmental stages, only relative (rather than absolute) intensity measurements are available. We agreed that such information is essential for establishing a more utilizable model and discussed it thoroughly in 3. Discussion and conclusion. From a theoretical perspective, we adopted assumptions from the previous literature and constructed a minimal model for a specific cell polarization phase to investigate the network's robustness, supported by five experimental groups and eight perturbed conditions in the *C. elegans* embryo.

> *The study extends its significance by examining how cells maintain pattern stability amid spatial parameter variations, which are common in natural systems due to extracellular and intracellular fluctuations. The authors found that in the 2-node network, varying individual parameters spatially disrupt the pattern, but stability is restored with compensatory variations. Additionally, the polarisation interface stabilises around the step transition between parameter values, making its localisation tunable. This suggests a potential biological mechanism where localisation might be regulated through signalling perception.*

We sincerely thank the editor(s) for the pertinent review!

> *Focusing on the C. elegans cell polarisation network, the authors propose a 5-node network based on an exhaustive literature review, summarised in a supplementary table. Using their computational pipeline, they identify several parameter sets capable of achieving stable polarisation and claim that their model replicates experimental behaviour, even when simulating mutants. They also found that among 34 possible network structures, the wild-type network with mutual inhibition is the only one that proves viable in the computational pipeline. Compared with previous studies, which typically considered only 2- or 3-node networks, this analysis provides a more complete and realistic picture of the signalling network behind polarisation in the C. elegans embryo. In particular, the model for C. elegans cell polarisation paves the way for further in silico experiments to investigate the role of the network structure over the polarisation dynamics. The authors suggest that the natural 5-node network of C. elegans is*

> *optimised for maintaining cell polarisation, demonstrating the elegance of evolution in finding the optimal network structure to achieve certain functions.*

We sincerely thank the editor(s) for the pertinent review!

> *Noteworthy limitations are also found in this work. To simplify the model for numerical exploration, the authors assume several reactions have equivalent dynamics, reducing the parameter space to three independent dimensions. While the authors briefly acknowledge this limitation in the "Discussion and Conclusion" section, further analysis might be required to understand the implications. For instance, it is not clear how the results depend on the particular choice of parameters. The authors showed that adding additional regulation might disrupt the polarised pattern, with the conclusion apparently depending on the strength of the regulation. Even for the 5-node wild-type network, which is the most robust, adding a strong enough self-activation of [A], as done in the 2-node network, will probably cause the polarised pattern to collapse as well.*

We sincerely thank the editor(s) for the comment!

Now we have thoroughly expanded our acknowledgment of the model's limitations in in 2. Results and 3. Discussion and conclusion. To rule out the equivalent dynamics assumption undermines our conclusions, we have added simulations showing that the cell polarization pattern stability does not depend on the exact strength of each regulation, provided the regulations on both sides are initially balanced as a whole (Fig. S5). Specifically, we used a Monte Carlo method to sample a wide range of various parameter values (i.e., γ, α, k_1, k_2, q_1, q_2 and $[X_c]$) for all nodes and regulations in simple 2-node network and *C. elegans* 5-node network, to achieve pattern stability. Under these conditions (i.e., without any reduction in the parameter space), single-sided self-regulation, single-sided additional regulation, and unequal system parameters still cause the stable polarized pattern to collapse, consistent with our conclusions in the simplified conditions with the parameter space reduced to three independent dimensions.

> *Additionally, the authors utilise parameter values that are unrealistic, fail to provide units for some of them, and assume unknown parameter values without justification. The model appears to have non-dimensionalised length but not time, resulting in a mix of dimensional and non-dimensional variables that can be confusing. Furthermore, they assume equal values for Hill coefficients and many parameters associated with activation and inhibition pathways, while setting inhibition intensity parameters to 1. These arbitrary choices raise concerns about the fidelity of the proposed model in representing the real system, as their selected values could potentially differ by many orders of magnitude from the actual parameters.*

We sincerely thank the editor(s) for the comment!

We apologize for the confusion. The non-dimensionalised parameter values are adopted from previous theoretical research [Seirin-Lee et al., Cells, 2020], which originates from the experimental measurement in [Goehring et al., J. Cell Biol., 2011; Goehring et al., Science, 2011]. With the *in silico* time set as 2 sec per step, now we have added the Supplemental Text justifying how the units are removed during non-dimensionalization. This demonstrates that the derived non-dimensionalized parameter in this paper achieves realistic values on the same order of magnitude as those observed in reality, confirming the fidelity of the proposed model in representing the real system.

The assumption of "equal values for Hill coefficients and many parameters associated with activation and inhibition pathways" is to reduce the parameter space for affordable computational cost. It is a widely-used strategy to fix Hill coefficients [Seirin-Lee et al., J.

Theor. Biol., 2015; Seirin-Lee, Bull. Math. Biol., 2021] and unify parameter values for different pathways in network research about both cell polarization [Marée et al., Bull. Math. Biol., 2006; Goehring et al., Science, 2011; Trong et al., New J. Phys., 2014] and other biological topics (e.g., plasmid transferring in the microbial community [Wang et al., Nat. Commun., 2020]), to control computational cost. Nevertheless, to rule out that the equivalent dynamics assumption undermines our conclusions, we have added simulations showing that the cell polarization pattern stability does not depend on the exact parameter values associated with activation and inhibition pathways, provided the regulations on both sides are initially balanced as a whole (Fig. S5). Specifically, we used a Monte Carlo method to sample a wide range of various parameter values (i.e_._, γ, α, k_1, k_2, q_1, q_2 and $[X_c]$) for all nodes and regulations in simple 2-node network and *C. elegans* 5-node network, to achieve pattern stability. Under these conditions (i.e., without any reduction in the parameter space), single-sided self-regulation, single-sided additional regulation, and unequal system parameters still cause the stable polarized pattern to collapse, consistent with our conclusions in the simplified conditions with the parameter space reduced to three independent dimensions.

To confirm the fidelity of the proposed model in representing the real system, we reproduced the qualitative and semi-quantitative phenomenon in three more experimental groups previously published (Section 2.5; Fig. S8) [Gotta et al., *Curr. Biol.*, 2001; Aceto et al., *Dev. Biol.*, 2006]. Combined with the original experiments (Section 2.5; Fig. 5; Fig. S7) [Hoege et al., Curr. Biol., 2010; Beatty et al., Development, 2010; Beatty et al., Development, 2013], now we have reproduced five experimental groups in total (two acting on LGL-1 and three on CDC-42), comprising eight perturbed conditions and using wild-type as the reference. These results effectively demonstrate how comprehensively the network structure and parameters capture the characteristics of the *C. elegans* embryo. We have also acknowledged the limitations of the current cell polarization model and provided, in 2. Results and 3. Discussion and conclusion, a detailed outline of potential model improvements.

It is worth noting that, although a strict match between numerical and realistic parameter values with consistent units is always helpful, a lot of notable pure numerical studies successfully unveil principles that help interpret [Ma et al., Cell, 2009] and synthesize real biological systems [Chau et al., Cell, 2012]. These studies suggest that numerical analysis in biological systems remains powerful, even when comprehensive experimental data from prior research are not fully available.

> *The definition of stability and its evaluation in the proposed pipeline might also be too narrow. Throughout the paper, the authors discuss the stability of the polarised pattern, checked by an exhaustive search of the parameter space where the system reaches a steady state with a polarised pattern instead of a homogeneous pattern. It is not clear if the stability is related to the linear stability analysis of the reaction terms, as conducted in Goehring et al. (Science, 2011), which could indicate if a homogeneous state exists and whether it is stable or unstable. The stability test is performed through a pipeline procedure where they always start from a polarised pattern described by their model and observe how it evolves over time. It is unclear if the conclusions depend on the chosen initial conditions. Particularly, it is unclear what would happen if the initial distribution of posterior molecules is not exactly symmetric with respect to the anterior molecules, or if the initial polarisation is not strong.*

We sincerely thank the editor(s) for the comment!

The definition of stability and its evaluation in the proposed pipeline consider two criteria: 1. The pattern is polarized; 2. The pattern is stable. Following simulations, figures, and videos (Fig. 1-6; Fig. S1-S5; Fig. S7-S9; Movie S1-S5) have sufficiently demonstrated that the parameters and networks set up capture the cell polarization dynamis regarding both the stable and unstable states very well.

Now we have added new simulation on alternative initial conditions. They demonstrating the necessity of a polarized initial pattern set up independently of the reaction-diffusion network during the establishment phase, probably through additional mechanisms such as the active actomyosin contractility and flow [Cuenca et al., Development, 2003; Gross et al., Nat. Phys., 2019]. Our conclusions (i.e., single-sided self-regulation, single-sided additional regulation, and unequal system parameters cause the stable polarized pattern to collapse) have little dependence on the chosen initial conditions as long as the unsymmetric initial patterns can set up a stable polarized pattern. A part of the simulations institutively show our conclusions still hold if the initial distribution of posterior molecules is not exactly symmetric with respect to the anterior molecules, or if the initial polarisation is not strong (Fig. S4 and Fig. S9).

> *Regarding the biological interpretation and relevance of the model, it overlooks some important aspects of the C. elegans polarisation system. The authors focus solely on a reaction-diffusion formulation to reproduce the polarisation pattern. However, the polarisation of the C. elegans zygote consists of two distinct phases: establishment and maintenance, with actomyosin dynamics playing a crucial role in both phases (see Munro et al., Dev Cell 2004; Shivas & Skop, MBoC 2012; Liu et al., Dev Biol 2010; Wang et al., Nat Cell Biol 2017). Both myosin and actin are crucial to maintaining the localisation of PAR proteins during cell polarisation, yet the authors neglect cortical flows during the establishment phase and any effects driven by myosin and actin in their model, failing to capture the system's complexity. How this affects the proposed model and conclusions about the establishment of the polarisation pattern needs careful discussion. Additionally, they assume that diffusion in the cytoplasm is infinitely fast and that cytoplasmic flows do not play any role in cell polarity. Finite cytoplasmic diffusion combined with cytoplasmic flows could compromise the stability of the anterior-posterior molecular distributions. The authors claim that cytoplasmic diffusion coefficients are two orders of magnitude higher than membrane diffusion coefficients, but they seem to differ by only one order of magnitude (Petrášek et al., Biophys. J. 2008). The strength of cytoplasmic flows has been quantified by a few studies, including Cheeks et al., and Curr Biol 2004.*

We sincerely thank the editor(s) for the comment!

Indeed, previous research highlighted the importance of convective cortical flow in orchestrating the localisation of PAR proteins during the establishment phase of polarisation formation [Goehring et al., J. Cell Biol., 2011; Rose et al., WormBook, 2014; Beatty et al., Development, 2013]. However, during the maintenance phase, the non-muscle myosin II (NMY-2) is regulated downstream by the PAR protein network rather than serving as the primary upstream factor controlling PAR protein localization [Goehring et al., J. Cell Biol., 2011; Rose et al., WormBook, 2014; Beatty et al., Development, 2013]. While some theoretical studies integrated both reaction-diffusion dynamics and the effects of myosin and actin [Tostevin, 2008; Goehring, Science, 2011], others focused exclusively on reaction-diffusion dynamics [Dawes et al., Biophys. J., 2011; Seirin-Lee et al., Cells, 2020]. We have now clarified the distinction between the establishment and maintenance phases in 1. Introduction, emphasized our research focus on the reaction-diffusion dynamics during the maintenance phase in 2. Results, and provided a discussion of the omitted actomyosin dynamics to foster a more comprehensive understanding in the future in 3. Discussion and conclusion. The effect of the establishment phase is studied as the initial condition for the cell polarization simulation solely governed by reaction-diffusion dynamics, with new simulations demonstrating the necessity of a polarized initial pattern set up independently of the reaction-diffusion network during the establishment phase, probably through additional mechanisms such as the active actomyosin contractility and flow [Cuenca et al., Development, 2003; Gross et al., Nat. Phys., 2019].

Cytoplasmic and membrane diffusion coefficients differ by two orders of magnitude according to previous experimental measurements on PAR-2 and PAR-6 [Goehring et al., J. Cell Biol., 2011; Lim et al., Cell Rep., 2021]. Many previous *C. elegans* cell polarization models have incorporated mass-conservation model combined with finite cytoplasmic diffusion, but this model description can lead to reverse spatial concentration distribution between the cell membrane and cytosol [Fig. 3 of Seirin-Lee et al., J. Theor. Biol., 2016; Fig. 2ab of Seirin-Lee et al., J. Math. Biol., 2020], disobeying experimental observation [Fig. 4A of Sailer et al., Dev. Cell, 2015; Fig. 1A of Lim et al., Cell Rep., 2021]. This implies that the infinite cytoplasmic diffusion, without precise experiment-based parameter assignment or accounting for other hidden biological processes (e.g., protein production and degradation), may be inappropriate in modeling the real spatial concentration distributions distinguished between the cell membrane and cytosol. To address this issue, some theoretical research incorporated protein production and degradation into their model, to acquire the consistent spatial concentration distribution between the cell membrane and cytosol [Tostevin et al., Biophys. J., 2008]. More definitive experimental data on the spatiotemporal changes in protein diffusion, production, and degradation are essential for providing a more realistic representation of cellular dynamics and enhancing the model's predictive power.

Now we have acknowledged the possibly overlooked aspects of the *C. elegans* polarisation system in 3. Discussion and conclusion, a detailed outline of potential model improvements. Those aspects include, but are not limited to, issues involving “neglect cortical flows” and the “diffusion in the cytoplasm is infinitely fast”. From a theoretical perspective, we adopted assumptions from the previous literature and constructed a minimal model for a specific cell polarization phase to investigate the network's robustness. The meaningful predictions of five experimental groups and eight perturbed conditions in the *C. elegans* embryo faithfully supports the biological interpretation and relevance of the model.

> *Although the authors compare their model predictions to experimental observations, particularly in reproducing mutant behaviours, they do not explicitly show or discuss these comparisons in detail. Diffusion coefficients and off-rates for some PAR proteins have been measured (Goehring et al., JCB 2011), but the authors seem to use parameter values that differ by many orders of magnitude, perhaps due to applied scaling. To ensure meaningful predictions, whether their proposed model captures the extensive published data should be evaluated. Various cellular/genetic perturbations have been studied to understand their effects on anterior-posterior boundary positioning. Testing these perturbations' responses in the model would be important. For example, comparing the intensity distribution of PAR-6 and PAR-2 with measurements during the maintenance phase by Goehring et al., JCB 2011, or comparing the normalised intensity of PAR-3 and PKC-3 from the model with those measured by Wang et al., Nat Cell Biol 2017, during establishment and maintenance phases (in both wild-type and cdc-42 (RNAi) zygotes) could provide insightful validation. Additionally, in the presence of active CDC-42, it has been observed that PAR-6 extends further into the posterior side (Aceto et al., Dev Biol 2006). Conducting such validation tests is essential to convince readers that the model accurately represents the actual system and provides insights into pattern formation during cell polarisation.*

We sincerely thank the editor(s) for the comment!

To provide more comprehensive validations and refinements to ensure the model accurately represents biological systems, we extensively reproduced the qualitative and semi-quantitative phenomenon in three more experimental groups previously published (Section 2.5; Fig. S8) [Gotta et al., Curr. Biol., 2001; Aceto et al., Dev. Biol., 2006]. Combined with the original experiments (Section 2.5; Fig. 5; Fig. S7) [Hoege et al., Curr. Biol., 2010; Beatty et al., Development, 2010; Beatty et al., Development, 2013], now we have reproduced five

experimental groups in total from published data, comprising eight perturbed conditions and using wild-type as the reference. We have also explicitly show the comparison between model predictions and experimental observations (including the mutant behaviors reproduction as well) in detail, by describing how “cell polarization pattern characteristics in simulation” responds to various cellular/genetic perturbations (Section 2.5; Fig. 5; Fig. S7 and S8). The original and new validation tests conducted can convince readers that the model accurately represents the actual system and provides insights into pattern formation during cell polarisation.

The diffusion coefficients for anterior and posterior molecular species were assigned according to previous experimental and theoretical research [Goehring et al., J. Cell Biol., 2011; Goehring et al., Science, 2011; Seirin-Lee et al., Cells, 2020]. The off-rates are assigned uniformly by searching viable parameter sets that can set up a network with cell polarization pattern stability. Now we have added simulations showing that the cell polarization pattern stability and response to network structure and parameter perturbation does not depend on the exact parameter values (incl., diffusion coefficients and off-rates), provided the parameter values on both sides are initially balanced as a whole (Fig. S5). Specifically, we used a Monte Carlo method to sample a wide range of various parameter values (i.e., γ, α, k_1, k_2, q_1, q_2 and $[X_c)$ for all nodes and regulations in simple 2-node network and *C. elegans* 5-node network, to achieve pattern stability. Under these conditions (i.e., without any reduction in the parameter space), single-sided self-regulation, single-sided additional regulation, and unequal system parameters still cause the stable polarized pattern to collapse, consistent with our conclusions in the simplified conditions with the parameter space reduced to three independent dimensions.

With the *in silico* time set as 2 sec per step, now we have added the Supplemental Text justifying how the units are removed during non-dimensionalization. This demonstrates that the derived non-dimensionalized parameter in this paper achieves realistic values on the same order of magnitude as those observed in reality, confirming the fidelity of the proposed model in representing the real system. We agreed that full experimental measurements of biological information are essential for establishing a more utilizable model and discussed it thoroughly in 3. Discussion and conclusion.

> *A clear justification, with references, for each network interaction between nodes in the five-node model is needed. Some of the activatory/inhibitory signals proposed by the authors have not been demonstrated (e.g. CDC-42 directly inhibiting CHIN-1). Table S2 provided by the authors is insufficient to justify each node-node interaction, requiring additional explanations. (See the review by Gubieda et al., Phil. Trans. R. Soc. B 2020, for a similar node network that differs from the authors' model.) Additionally, the intensity distributions of cortical PAR-3 and PKC-3 seem to vary significantly during both establishment and maintenance phases (Wang et al., Nat Cell Biol 2017), yet the authors consider the PAR-3/PAR-6/PKC-3 as a single complex. The choices in the model should be justified, as the presence or absence of clustering of these PAR proteins can be crucial during cell polarisation (Wang et al., Nat Cell Biol 2017; Dawes & Munro, Biophys J 2011).*

We sincerely thank the editor(s) for the comment!

Now we have acknowledged the limitations of the current cell polarization model and provided, in 2. Results and 3. Discussion and conclusion, a detailed outline of potential model improvements. The limitations include, but are not limited to, issues involving “each network interaction between nodes” and the “consider the PAR-3/PAR-6/PKC-3 as a single complex”, in which the former one relies on experimental measurements of biological information. However, comprehensive experimental measurement data on every molecular species, their interactions, and each species’ intensity distribution in space and time were not fully available from prior research. Refinement is lacking for some of these interactions,

potentially requiring years of additional experimentation. Moreover, for certain species at specific developmental stages, only relative (rather than absolute) intensity measurements are available. We agreed that such information is essential for establishing a more utilizable model and discussed it thoroughly in 3. Discussion and conclusion.

In consistent with previous modeling efforts [Goehring et al., Science, 2011; Gross et al., Nat. Phys., 2019; Lim et al., Cell Rep., 2021], our model treats the PAR-3/PAR-6/PKC-3 complex as a single entity for simplification, thus neglecting the potentially distinct spatial distributions of each single molecular species. We agree that a more comprehensive model, capable of resolving the individual localization patterns of these anterior PAR proteins, would be a valuable future direction. From a theoretical perspective, we adopted assumptions from the previous literature and constructed a minimal model for a specific cell polarization phase to investigate the network's robustness, supported by five experimental groups and eight perturbed conditions in the *C. elegans* embryo.

> *In summary, the authors successfully demonstrate the importance of compensatory actions in maintaining polarisation robustness. Their computational pipeline offers valuable insights into the dynamics of reaction-diffusion networks. However, the lack of detailed experimental validation and realistic parameter estimation limits the model's applicability to real biological systems. While the study provides a solid foundation, further work is needed to fully characterise and validate the model in natural contexts. This work has the potential to significantly impact the field by providing a new perspective on the robustness of cell polarisation networks.*

We sincerely thank the editor(s) for the pertinent summary!

To provide a more comprehensive validation against experimental data and model parameters, three more groups of the qualitative and semi-quantitative phenomenon regarding CDC-42 are reproduced based on previously published experiments (Section 2.5; Fig. S8) [Gotta et al., Curr. Biol., 2001; Aceto et al., Dev. Biol., 2006]. Combined with the original experiments (Section 2.5; Fig. 5; Fig. S7) [Hoege et al., Curr. Biol., 2010; Beatty et al., Development, 2010; Beatty et al., Development, 2013], now we have reproduced five experimental groups in total, comprising eight perturbed conditions and using wild-type as the reference.

With the in silico time set as 2 sec per step, now we have added the Supplemental Text justifying how the units are removed during non-dimensionalization. This demonstrates that the derived non-dimensionalized parameter in this paper achieves realistic values on the same order of magnitude as those observed in reality, confirming the fidelity of the proposed model in representing the real system. Together with the reproduction of five experimental groups (eight perturbed conditions with wild-type as the reference), the model’s applicability to real biological systems in natural contexts are are fully characterised and validated.

> *The computational pipeline developed could be a valuable tool for further in silico experiments, allowing researchers to explore the dynamics of more complex networks. To maximise its utility, the model needs comprehensive validation and refinement to ensure it accurately represents biological systems. Addressing these limitations, particularly the need for more detailed experimental validation and realistic parameter choices, will enhance the model's predictive power and its applicability to understanding cell polarisation in natural systems.*

We sincerely thank the editor(s) for the comment!

To provide more comprehensive validations and refinements to ensure the model accurately represents biological systems, we extensively reproduced the qualitative and semi-

quantitative phenomenon in three more experimental groups previously published (Section 2.5; Fig. S8) [Gotta et al., Curr. Biol., 2001; Aceto et al., Dev. Biol., 2006]. Combined with the original experiments (Section 2.5; Fig. 5; Fig. S7) [Hoege et al., Curr. Biol., 2010; Beatty et al., Development, 2010; Beatty et al., Development, 2013], now we have reproduced five experimental groups in total from published data, comprising eight perturbed conditions and using wild-type as the reference. We have also explicitly show the comparison between model predictions and experimental observations (including the mutant behaviors reproduction as well) in detail, by describing how "cell polarization pattern characteristics in simulation" responds to various cellular/genetic perturbations (Section 2.5; Fig. 5; Fig. S7 and S8).

With the *in silico* time set as 2 sec per step, now we have added the Supplemental Text justifying how the units are removed during non-dimensionalization. This demonstrates that the derived non-dimensionalized parameter in this paper achieves realistic values on the same order of magnitude as those observed in reality, confirming the fidelity of the proposed model in representing the real system. Together with the reproduction of five experimental groups (eight perturbed conditions with wild-type as the reference), the model's predictive power and its applicability to understanding cell polarisation in natural systems are enhanced.

Now we have added simulations showing that the cell polarization pattern stability and response to network structure and parameter perturbation does not depend on the exact parameter values (incl., diffusion coefficients, basal off-rates and inhibition intensity), provided the parameter values on both sides are initially balanced as a whole (Fig. S5). Specifically, we used a Monte Carlo method to sample a wide range of various parameter values (i.e., γ, α, k_1, k_2, q_1, q_2 and $[X_c)$ for all nodes and regulations in simple 2-node network and *C. elegans* 5-node network, to achieve pattern stability. Under these conditions (i.e., without any reduction in the parameter space), single-sided self-regulation, single-sided additional regulation, and unequal system parameters still cause the stable polarized pattern to collapse, consistent with our conclusions in the simplified conditions with the parameter space reduced to three independent dimensions.

> ***Recommendations for the Authors:***
>
> *(1) Parameterisation and Model Validation: The authors utilise parameter values that lack realism and fail to provide units for some of them, which can lead to confusion. For instance, the length of the cell is set to 0.5 without clear justification, raising questions about the scale used. Additionally, there's a mix of dimensional and non-dimensional variables, potentially complicating interpretation. Furthermore, arbitrary choices such as equal Hill coefficients and setting inhibition intensity parameters to 1 raise concerns about model fidelity. To ensure meaningful predictions, the authors should validate their model against extensive published data, including cellular/genetic perturbations. For example, comparing intensity distributions of PAR proteins measured during maintenance phases by Goehring et al., JCB 2011, and those obtained from the model could provide valuable validation. Similarly, comparisons with data from Wang et al., Nat Cell Biol 2017, on wild-type and cdc-42 (RNAi) zygotes, as well as observations from Aceto et al., Dev Biol 2006, on PAR-6 extension in the presence of active CDC-42, would strengthen the model's validity. Such validation tests are essential for convincing readers that the model accurately represents the actual system and can provide insights into pattern formation during cell polarisation.*

We sincerely thank the editor(s) and referee(s) for the helpful suggestion!

Now we have added a new section, Parameter Nondimensionalization and Order of Magtitude Consistency, into Supplemental Text. In this section, we introduced how we

adopted the parameter nondimensionalization and value assignments from previous works [Goehring et al., J. Cell Biol., 2011; Goehring et al., Science, 2011; Seirin-Lee et al., Cells, 2020]. We listed four examples (i.e., evolution time, membrane diffusion coefficient, basal off-rate, and inhibition intensity) to show the consistency in order of magtitude between numerical and realistic values.

The assumption of "equal Hill coefficients" is to reduce the parameter space for an affordable computational cost. It is a widely-used strategy to fix Hill coefficients [Seirin-Lee et al., J. Theor. Biol., 2015; Seirin-Lee, Bull. Math. Biol., 2021] in network research, to control computational cost. Besides, setting inhibition intensity parameters to 1 is for determining a numerical scale. Now we have added simulations showing that the cell polarization pattern stability does not depend on the exact parameter values associated with activation and inhibition pathways, provided the regulations on both sides are initially balanced as a whole (Fig. S5). Specifically, we used a Monte Carlo method to sample a wide range of various parameter values (i.e., γ, α, k_1, k_2, q_1, q_2 and $[X_c]$) for all nodes and regulations in simple 2-node network and *C. elegans* 5-node network, to achieve pattern stability. Under these conditions (i.e., without any reduction in the parameter space), single-sided self-regulation, single-sided additional regulation, and unequal system parameters still cause the stable polarized pattern to collapse, consistent with our conclusions in the simplified conditions with the parameter space reduced to three independent dimensions.

To confirm the fidelity of the proposed model in representing the real system, we reproduced the qualitative and semi-quantitative phenomenon in three more experimental groups previously published (Section 2.5; Fig. S8) [Gotta et al., Curr. Biol., 2001; Aceto et al., Dev. Biol., 2006]. Combined with the original experiments (Section 2.5; Fig. 5; Fig. S7) [Hoege et al., Curr. Biol., 2010; Beatty et al., Development, 2010; Beatty et al., Development, 2013], now we have reproduced five experimental groups in total (two acting on LGL-1 and three on CDC-42), comprising eight perturbed conditions and using wild-type as the reference. These results effectively demonstrate how comprehensively the network structure and parameters capture the characteristics of the *C. elegans* embryo. We have also acknowledged the limitations of the current cell polarization model and provided, in 2. Results and 3. Discussion and conclusion, a detailed outline of potential model improvements.

It is worth noting that, although a strict match between numerical and realistic parameter values with consistent units is always helpful, a lot of notable pure numerical studies successfully unveil principles that help interpret [Ma et al., Cell, 2009] and synthesize real biological systems [Chau et al., Cell, 2012]. These studies suggest that numerical analysis in biological systems remains powerful, even when comprehensive experimental data from prior research are not fully available.

> *(2) Parameter Changes: It is not clear how the parameters change as more complicated networks are explored, and how this affects the comparison between the simple and complete model. Clarification on this point would be beneficial.*

We sincerely thank the editor(s) and referee(s) for the helpful suggestion!

The computational pipeline in Section 2.1 is generalized for all reaction-diffusion networks, including the simple and complete ones studied in this paper. The parameter changes included two parts: 1. The mutual activation in the anterior (none for the simple 2-node network and q<sub2 for the complete 5-node network); 2. The viable parameter sets (122 sets for the simple 2-node network and 602 sets for the complete 5-node network). Now we have explicitly clarified those differences:

Those differences don't affect the comparison between the simple and complete models. Now we have added comprehensive comparisons between the simple and complete models about 1. How they respond to alternative initial conditions consistently (Fig. S2). 2. How they

respond to alternative single modifications consistently (Fig. S4 and S9), even when the parameters (i.e., γ, α, k_1, k_2, q_1, q_2 and [X_c) are assigned with various values concerning all nodes and regulations (Fig. S5).

(3) Exploration of Model Parameter Space: In the two-node dual antagonistic model, the authors observe that the cell polarisation pattern is unstable for different systems (Fig. 1). However, it remains uncertain whether this instability holds true for the entire model parameter space. Have the authors thoroughly screened the full model parameter space to support their statements? It would be beneficial for the authors to provide clarification on the extent of their exploration of the model parameter space to ensure the robustness of their conclusions.

We sincerely thank the editor(s) and referee(s) for the helpful suggestion!

The trade-off between considered parameter space and computational cost is a long-term challenge in network study as there are always numerous combinations of network nodes, edges, and parameters [Ma et al., Cell, 2009; Chau et al., Cell, 2012]. The computational pipeline in Section 2.1 generalized for all reaction-diffusion networks exerts two strategies to limit the computational cost and set up a basic network reference: 1. Dimension Reduction (Strategy 1) - Unifying the parameter values for different nodes and different edges within the same regulatory type to minimize the unidentical parameter numbers into 3; 2: Parameter

Space Confinement (Strategy 2): Enumerating the dimensionless parameter set $\Omega(\gamma, k_1, q_2)$ on a

three-dimensional (3D) grid confined by $\gamma \in [0,0.05]$ in steps $\Delta\gamma = 0.001$, $k_1 \in [0,5]$ in steps $\Delta k_1 = 0.05$, and in steps .

In the early stage of our project, we tried to explore “the entire model parameter space” as indicated by the reviewer. We first tried to use the Monte Carlo method to find parameter solutions in an open parameter space and with all parameter values allowed to be different. However, such a process is full of randomness and is computationally expensive (taking months to search viable parameter sets but still unable to profile the continuous viable parameter space; the probability of finding a viable parameter set is no higher than 0.02%, making it very hard to profile a continuous viable parameter space). Now we clearly can see the viable parameter space is a thin curved surface where all parameters have to satisfy a critical balance (Fig. 3a, b, Fig. 5e, f). This is why we exert a typical strategy for dimension reduction in network research in both cell polarization [Marée et al., Bull. Math. Biol., 2006; Goehring et al., Science, 2011; Trong et al., New J. Phys., 2014] and other biological topics (e.g., plasmid transferring in the microbial community [Wang et al., *Nat. Commun.*, 2020]), i.e., unifying the parameter values for different nodes and different edges within the same regulatory type.

Additionally, the curved surface for viable parameter space can be extended to infinite as long as the parameter balance is achieved (Fig. 3a, b, Fig. 5e, f), it is impossible or unnecessary to explore “the entire model parameter space”. Setting up a confined parameter region near the original point for parameter enumeration can help profile the continuous viable parameter space, which is sufficient for presenting the central conclusion of this paper – that is - the network structure and parameter need to satisfy a balance for stable cell polarization.

To support a comprehensive study considering all kinds of reference and perturbed networks, we have maximized the parameter domain size by exhausting all the computational research we can access, including 400-500 Intel(R) Core(TM) E5-2670v2 and Gold 6132 CPU on the server (High-Performance Computing Platform at Peking University) and 5 Intel(R) Core(TM) i9-14900HX CPU on personal computers.

To make it certain that instability holds true when the model parameter space is extended, we add a comprehensive comparison between the simple and complete models about how their instability occurs consistently even when the parameters (i.e., γ, α, k_1, k_2, q_1, q_2 and $[X_c]$) are assigned with various values concerning all nodes and regulations, searched by the Monte Carlo method (Fig. S5).

> *(4) Sensitivity of Numerical Solutions to Initial Conditions: Are the numerical solutions in both models sensitive to the chosen initial condition? What results do the models provide if uniform initial distributions were utilised instead?*

We sincerely thank the editor(s) and referee(s) for the comments!

To investigate both the simple network and the realistic network consisting of various node numbers and regulatory pathways [Goehring et al., Science, 2011; Lang et al., Development, 2017], we propose a computational pipeline for numerical exploration of the dynamics of a given reaction-diffusion network's dynamics, specifically targeting the maintenance phase of stable cell polarization after its initial establishment [Motegi et al., Nat. Cell Biol., 2011; Goehring et al., Science, 2011; Seirin-Lee et al., Cells, 2020].

Now we have added new simulations and explanations for the sensitivity of numerical solutions to initial conditions. For both models, a uniform initial distribution leads to a homogeneous pattern while a Gaussian noise distribution leads to a multipolar pattern. In contrast, an initial polarized distribution (even with shifts in transition planes, weak polarization, or asymmetric curve shapes between the two molecular species) can maintain cell polarization reliably.

> *(5) Initial Conditions and Stability Tests: In Figure 1, the authors discuss the stability of the basic two-node network (a) upon modifications in (b-d). The stability test is performed through a pipeline procedure in which they always start from a polarised pattern described by Equation (4) and observe how the pattern evolves over time. It would be beneficial to explore whether the stability test depends on this specific initial condition. For instance, what would happen if the posterior molecules have an initial distribution of 1/(1+e^(-10x)), which is not exactly symmetric with respect to the anterior molecules' distribution of 1-1/(1+e^(-20x))? Additionally, if the initial polarisation is not as strong, for example, with the anterior molecules having a distribution of 10-1/(1+e^(-20x)) and the posterior molecules having a distribution of 9+1/(1+e^(-20x)), how would this affect the results?*

We sincerely thank the editor(s) and referee(s) for the constructive advice!

Now we have added comprehensive comparisons between the simple and complete models about how they respond to alternative initial conditions consistently (Fig. S4, Fig. S9). The successful cell polarization pattern requests an initial polarized pattern, but its following stability and response to perturbation depend very little on the specific form of the initial polarized pattern. All the conditions mentioned by the reviewer have been included.

> *(6) Stability Analysis: Throughout the paper, the authors discuss the stability of the polarised pattern. The stability is checked by an exhaustive search of the parameter space, ensuring the system reaches a steady state with a polarised pattern instead of a homogeneous pattern. It would be beneficial to explore if this stability is related to a linear stability analysis of the model parameters, similar to what was conducted in Reference [18], which can determine if a homogeneous state exists and whether it is stable or unstable. Including such an analysis could provide deeper insights into the system's stability and validate its robustness.*

We sincerely thank the editor(s) and referee(s) for the comments!

We agree that the linear stability analysis can potentially offer additional insights into polarized pattern behavior. However, this approach often requests the aid of numerical solutions and is therefore not entirely independent [Goehring et al., Science, 2011]. Over the past decade, numerical simulations have consistently proven to be a reliable and sufficient approach for studying network dynamics, spanning from *C. elegans* cell polarization [Tostevin et al., *Biophys. J*, 2008; Blanchoud et al., Biophys. J, 2015; Seirin-Lee, Dev. Growth Differ., 2020] to topics in metazoon [Chau et al., Cell, 2012; Qiao et al., eLife, 2022; Sokolowski et al., arXiv, 2023]. Numerous purely numerical studies have successfully unveiled principles that help interpret [Ma et al., Cell, 2009] and synthesized real biological systems [Chau et al., Cell, 2012], independent of additional mathematical analysis. Thus, we leverage our numerical framework to address the cell polarization problems cell polarization problems in this paper.

To confirm the reliability of stability checked by an exhaustive search of the parameter space, now we reproduce the qualitative and semi-quantitative phenomenon in three more experimental groups previously published (Section 2.5; Fig. S8) [Gotta et al., Curr. Biol., 2001; Aceto et al., Dev. Biol., 2006]. Combined with the original experiments (Section 2.5; Fig. 5; Fig. S7) [Hoege et al., Curr. Biol., 2010; Beatty et al., Development, 2010; Beatty et al., Development, 2013], we reproduce five experimental groups in total (two acting on LGL-1 and three acting on CDC-42), comprising eight perturbed conditions and using wild-type as the reference.

To confirm the robustness of our conclusions regarding the system's stability, now we add comprehensive comparisons between the simple and complete models about 1. How they respond to alternative initial conditions consistently (Fig. S4; Fig. S9). 2. How they respond to alternative single modifications consistently, even when the parameters (i.e., γ, α, k_1, k_2, q_1, q_2 and $[X_c]$) are assigned with various values concerning all nodes and regulations (Fig. S5).

> *(7) Interface Position Determination: In Figure 4, the authors demonstrate that by using a spatially varied parameter, the position of the interface can be tuned. Particularly, the interface is almost located at the step where the parameter has a sharp jump. However, in the case of a homogeneous parameter (e.g., Figure 4(a)), the system also reaches a stable polarised pattern with the interface located in the middle (x = 0), similar to Figure 4(b), even though the homogeneous parameter does not contain any positional information of the interface. It would be helpful to clarify the difference between Figure 4(a) and Figure 4(b) in terms of the interface position determination.*

We sincerely thank the editor(s) and referee(s) for the comments!

The case of a homogeneous parameter (e.g., Fig. 4a), in which the system also reaches a stable polarised pattern with the interface located in the middle (x = 0), is just a reference adopted from Fig. 1a to show that the inhomogeneous positional information in Fig. 4b can achieve a similar stable polarised pattern.

Now we clarify the interface position determination to Section 2.4 to improve readability. Moreover, it is marked with grey dashed line in all the patterns in Fig. 4 and Fig. 6 to highlight the importance of inhomogeneous parameters on interface localization.

> *(8) Presented Comparison with Experimental Observations: The comparison with experimental observations lacks clarity. It isn't clear that the model "faithfully recapitulates" the experimental observations (lines 369-370). We recommend discussing and showing these comparisons more carefully, highlighting the expectations and similarities.*

We sincerely thank the editor(s) and referee(s) for the constructive suggestion!

Now we remove the word “faithfully” and highlight the expectations and similarities of each experimental group by describing “cell polarization pattern characteristics in simulation: …”.

> *(9) Validation of Model with Experimental Data: Given the extensive number of model parameters and the uncertainty of their values, it is essential for the authors to validate their model by comparing their results with experimental data. While C. elegans polarisation has been extensively studied, the authors have yet to utilise existing data for parameter estimation and model validation. Doing so would considerably strengthen their study.*

We sincerely thank the editor(s) and referee(s) for the constructive suggestion!

To utilise existing data for parameter estimation, now we add a new section, Parameter Nondimensionalization and Order of Magtitude Consistency, into Supplemental Text. In this section, we introduced how we adopted the parameter nondimensionalization and value assignments from previous works [Goehring et al., J. Cell Biol., 2011; Goehring et al., Science, 2011; Seirin-Lee et al., Cells, 2020]. We listed four examples (i.e., evolution time, membrane diffusion coefficient, basal off-rate, and inhibition intensity) to show the consistency in order of magtitude between numerical and realistic values.

To utilise existing data for model validation, now we reproduce the qualitative and semi-quantitative phenomenon in three more experimental groups previously published (Section 2.5; Fig. S8) [Gotta et al., Curr. Biol., 2001; Aceto et al., Dev. Biol., 2006]. Combined with the original experiments (Section 2.5; Fig. 5; Fig. S7) [Hoege et al., Curr. Biol., 2010; Beatty et al., Development, 2010; Beatty et al., Development, 2013], we reproduce five experimental groups in total (two acting on LGL-1 and three acting on CDC-42), comprising eight perturbed conditions and using wild-type as the reference.

Also, we acknowledge the limitations of the current cell polarization model and provided, in 3. Discussion and conclusion, a detailed outline of potential model improvements. The limitations include, but are not limited to, issues involving “extensive number of model parameters” and “uncertainty of their values”, both of which rely on experimental measurements of biological information. However, comprehensive experimental measurement data on every molecular species, their interactions, and each species’ intensity distribution in space and time were not fully available from prior research. Refinement is lacking for some of these interactions, potentially requiring years of additional experimentation. Moreover, for certain species at specific developmental stages, only relative (rather than absolute) intensity measurements are available. We agreed that such information is essential for establishing a more utilizable model and discussed it thoroughly in 3. Discussion and conclusion. From a theoretical perspective, we adopted assumptions from the previous literature and constructed a minimal model for a specific cell polarization phase to investigate the network's robustness, supported by five experimental groups and eight perturbed conditions with wild-type as a reference in the *C. elegans* embryo.

> *(10) Enhancing Model Accuracy by Considering Cortical Flows: The authors are encouraged to include cortical flows in their cell polarisation model, as these flows are known to be pivotal in the process. Although the current model successfully predicts cell polarisation without accounting for cortical flows, research has demonstrated their significant role in polarisation formation. By incorporating cortical flows, the model would provide a more thorough and precise representation of the biological process. Furthermore, previous studies, such as those by Goehring et al. (References 17 and 18), highlight the importance of convective actin flow in initiating polarisation. It would be valuable for the authors to address the contribution of convection with actin flow to the*

> *establishment of the polarisation pattern. The polarisation of the C. elegans zygote progresses through two distinct phases: establishment and maintenance, both heavily influenced by actomyosin dynamics. Works by Munro et al. (Dev Cell 2004), Shivas & Skop (MBoC 2012), Liu et al. (Dev. Biol. 2010), and Wang et al. (Nat Cell Biol 2017) underscore the critical roles of myosin and actin in orchestrating the localisation of PAR proteins during cell polarisation. To enhance the fidelity of their model, we recommend that the authors either integrate cortical flows and consider the effects driven by myosin and actin, or provide a discussion on the repercussions of omitting these dynamics.*

We sincerely thank the editor(s) and referee(s) for the comment!

Indeed, previous research highlighted the importance of convective cortical flow in orchestrating the localisation of PAR proteins during the establishment phase of polarisation formation [Goehring et al., J. Cell Biol., 2011; Rose et al., WormBook, 2014; Beatty et al., Development, 2013]. However, during the maintenance phase, the non-muscle myosin II (NMY-2) is regulated downstream by the PAR protein network rather than serving as the primary upstream factor controlling PAR protein localization. While some theoretical studies integrated both reaction-diffusion dynamics and the effects of myosin and actin [Tostevin et al., Biophys J, 2008; Goehring et al, Science, 2011], others focused exclusively on reaction-diffusion dynamics [Dawes et al., Biophys. J., 2011; Seirin-Lee et al., Cells, 2020]. Now we clarify the distinction between the establishment and maintenance phases, emphasize our research focus on the reaction-diffusion dynamics during the maintenance phase, and provide a discussion of these omitted dynamics to foster a more comprehensive understanding in the future, as suggested.

> *(11) Further Justification of Network Interactions: The authors should provide additional explanations, supported by empirical evidence, for the network interactions assumed in their model. This includes both node-node interactions and the rationale behind protein complex formations. Some of the proposed interactions lack empirical validation, as noted in studies such as Gubieda et al., Phil. Trans. R. Soc. B 2020. Additionally, discrepancies in protein intensity distributions, as observed in Wang et al., Nat Cell Biol 2017, should be addressed, particularly concerning the consideration of the PAR-3/PAR-6/PKC-3 complex as a single entity. Justifying these choices is crucial for ensuring the model's credibility and alignment with experimental findings.*

We sincerely thank the editor(s) and referee(s) for the helpful advice!

In consistency with previous modeling efforts [Goehring et al., Science, 2011; Gross et al., Nat. Phys., 2019; Lim et al., Cell Rep., 2021], our model treats the PAR-3/PAR-6/PKC-3 complex as a single entity for simplification, thus neglecting the potentially distinct spatial distributions of each single molecular species.

Now we acknowledge the limitations of the current cell polarization model and provided, in 3. Discussion and conclusion, a detailed outline of potential model improvements. The limitations include, but are not limited to, issues involving “node-node interactions” and “discrepancies in protein intensity distributions”, both of which rely on experimental measurements of biological information. However, comprehensive experimental measurement data on every molecular species, their interactions, and each species’ intensity distribution in space and time were not fully available from prior research. Refinement is lacking for some of these interactions, potentially requiring years of additional experimentation. Moreover, for certain species at specific developmental stages, only relative (rather than absolute) intensity measurements are available. We agreed that such information is essential for establishing a more utilizable model and discussed it thoroughly in 3. Discussion and conclusion.

To ensure the model's credibility and alignment with experimental findings, now we reproduce the qualitative and semi-quantitative phenomenon in three more experimental groups previously published (Section 2.5; Fig. S8) [Gotta et al., Curr. Biol., 2001; Aceto et al., Dev. Biol., 2006]. Combined with the original experiments (Section 2.5; Fig. 5; Fig. S7) [Hoege et al., Curr. Biol., 2010; Beatty et al., Development, 2010; Beatty et al., Development, 2013], now we have reproduced five experimental groups in total (two acting on LGL-1 and three on CDC-42), comprising eight perturbed conditions and using wild-type as the reference.

> *(12) Further Justification of Node-Node Network Interactions: The authors should provide further justification for the node-node network interactions assumed in their study. To the best of our knowledge, some of the node-node interactions proposed have not yet been empirically demonstrated. Providing additional explanations for these interactions would enhance the credibility of the model and ensure its alignment with empirical evidence.*

We sincerely thank the editor(s) and referee(s) for the helpful advice!

Now we acknowledge the limitations of the current cell polarization model and provided, in 3. Discussion and conclusion, a detailed outline of potential model improvements. The limitations include, but are not limited to, issues involving “node-node network interactions”, which rely on experimental measurements of biological information. However, comprehensive experimental measurement data on every molecular species, their interactions, and each species’ intensity distribution in space and time were not fully available from prior research. Refinement is lacking for some of these interactions, potentially requiring years of additional experimentation. Moreover, for certain species at specific developmental stages, only relative (rather than absolute) intensity measurements are available. We agreed that such information is essential for establishing a more utilizable model and discussed it thoroughly in 3. Discussion and conclusion.

To enhance the credibility of the model and ensure its alignment with empirical evidence, we reproduced the qualitative and semi-quantitative phenomenon in three more experimental groups previously published (Section 2.5; Fig. S8) [Gotta et al., Curr. Biol., 2001; Aceto et al., Dev. Biol., 2006]. Combined with the original experiments (Section 2.5; Fig. 5; Fig. S7) [Hoege et al., Curr. Biol., 2010; Beatty et al., Development, 2010; Beatty et al., Development, 2013], now we have reproduced five experimental groups in total (two acting on LGL-1 and three on CDC-42), comprising eight perturbed conditions and using wild-type as the reference.

> *(13) Justification for Network Interactions and Protein Complexes: The authors must provide clear justifications, supported by references, for each network interaction between nodes in the five-node model. Some of the activatory/inhibitory signals proposed lack empirical validation, such as CDC-42 directly inhibiting CHIN-1. The provided Table S2 is insufficient to justify these interactions, necessitating additional explanations. Reviewing relevant literature, such as the work by Gubieda et al., Phil. Trans. R. Soc. B 2020, may offer insights into similar node networks. Furthermore, the authors should address discrepancies in protein intensity distributions, as observed in studies like Wang et al., Nat Cell Biol 2017. Specifically, the authors consider the PAR-3/PAR-6/PKC-3 complex as a single entity despite potential differences in their distributions. Justification for this choice is essential, particularly considering the importance of clustering dynamics during cell polarisation, as demonstrated by Wang et al., Nat Cell Biol 2017, and Dawes & Munro, Biophys J 2011.*

We sincerely thank the editor(s) and referee(s) for the helpful advice!

In consistent with previous modeling efforts [Goehring et al., Science, 2011; Gross et al., Nat. Phys., 2019; Lim et al., Cell Rep., 2021], our model treats the PAR-3/PAR-6/PKC-3 complex as a single entity for simplification, thus neglecting the potentially distinct spatial distributions of each single molecular species. Besides, the inhibition of CHIN-1 from CDC-42, which recruits cytoplasmic PAR-6/PKC-3 to form a complex, may act indirectly to restrict CHIN-1 localization through phosphorylation [Sailer et al., Dev. Cell, 2015; Lang et al., Development, 2017].

Now we acknowledge the limitations of the current cell polarization model and provided, in 3. Discussion and conclusion, a detailed outline of potential model improvements. The limitations include, but are not limited to, issues involving “each network interaction between nodes in the five-node model” and “discrepancies in protein intensity distributions”, both of which rely on experimental measurements of biological information. However, comprehensive experimental measurement data on every molecular species, their interactions, and each species’ intensity distribution in space and time were not fully available from prior research. Refinement is lacking for some of these interactions, potentially requiring years of additional experimentation. Moreover, for certain species at specific developmental stages, only relative (rather than absolute) intensity measurements are available. We agreed that such information is essential for establishing a more utilizable model and discussed it thoroughly in 3. Discussion and conclusion. From a theoretical perspective, we adopted assumptions from the previous literature and constructed a minimal model for a specific cell polarization phase to investigate the network's robustness, supported by five experimental groups and eight perturbed conditions with wild-type as a reference in the *C. elegans* embryo.

> *(14) Incorporating Cytoplasmic Dynamics into the Model: The authors assume infinite cytoplasmic diffusion and neglect the role of cytoplasmic flows in cell polarity, which may oversimplify the model. Finite cytoplasmic diffusion combined with flows could potentially compromise the stability of anterior-posterior molecular distributions, affecting the accuracy of the model's predictions. The authors claim a significant difference between cytoplasmic and membrane diffusion coefficients, but the actual disparity seems smaller based on data from Petrášek et al., Biophys. J. 2008. For example, cytosolic diffusion coefficients for NMY-2 and PAR-2 differ by less than one order of magnitude. Additionally, the strength of cytoplasmic flows, as quantified by studies such as Cheeks et al., and Curr Biol 2004, should be considered when assessing the impact of cytoplasmic dynamics on polarity stability. Incorporating finite cytoplasmic diffusion and cytoplasmic flows into the model could provide a more realistic representation of cellular dynamics and enhance the model's predictive power.*

We sincerely thank the editor(s) and referee(s) for the comment!

Cytoplasmic and membrane diffusion coefficients differ by two orders of magnitude according to previous experimental measurements on PAR-2 and PAR-6 [Goehring et al., J. Cell Biol., 2011; Lim et al., Cell Rep., 2021]. Many previous C. *elegans* cell polarization models have incorporated mass-conservation model combined with finite cytoplasmic diffusion, but this model description can lead to reverse spatial concentration distribution between the cell membrane and cytosol [Fig. 3 of Seirin-Lee et al., J. Theor. Biol., 2016; Fig. 2ab of Seirin-Lee et al., J. Math. Biol., 2020], disobeying experimental observation [Fig. 4A of Sailer et al., Dev. Cell, 2015; Fig. 1A of Lim et al., Cell Rep., 2021]. This implies that the infinite cytoplasmic diffusion, without precise experiment-based parameter assignment or accounting for other hidden biological processes (e.g., protein production and degradation), may be inappropriate in modeling the real spatial concentration distributions distinguished between the cell membrane and cytosol. To address this issue, some theoretical research incorporated protein production and degradation into their model, to acquire the consistent spatial concentration distribution between the cell membrane and cytosol [Tostevin et al., Biophys. J., 2008]. More

definitive experimental data on the spatiotemporal changes in protein diffusion, production, and degradation are essential for providing a more realistic representation of cellular dynamics and enhancing the model's predictive power.

Cytoplasmic flows indeed play an unneglectable role in cell polarity during the establishment phase [Kravtsova et al., Bull. Math. Biol., 2014], which creates a spatial gradient of actomyosin contractility and directs PAR-3/PKC-3/PAR-6 to the anterior membrane by cortical flow [Rose et al., WormBook, 2014; Lang et al., Development, 2017]. However, during the maintenance phase, the non-muscle myosin II (NMY-2) is regulated downstream by the PAR protein network rather than serving as the primary upstream factor controlling PAR protein localization [Goehring et al., J. Cell Biol., 2011; Rose et al., WormBook, 2014; Geβele et al., Nat. Commun., 2020]. While some theoretical studies integrated both reaction-diffusion dynamics and the effects of myosin and actin [Tostevin, 2008; Goehring, Science, 2011], others focused exclusively on reaction-diffusion dynamics [Dawes et al., Biophys. J., 2011; Seirin-Lee et al., Cells, 2020]. We now emphasize our research focus on the reaction-diffusion dynamics during the maintenance phase, so the dynamics between NMY-2 and PAR-2 are not included. We have also provided a discussion of the simplified cytoplasmic diffusion and omitted cytoplasmic flows to foster a more comprehensive understanding in the future.

> *(15) Explanation of Lethality References: On page 13, the authors mention lethality without adequately explaining why they are drawing connections with lethality experimental data.*

We sincerely thank the editor(s) and referee(s) for the comment!

It is well-known that cell polarity loss in *C. elegans* zygote will lead to symmetric cell division, which brings out the more symmetric allocation of molecular-to-cellular contents in daughter cells; this will result in abnormal cell size, cell cycle length, and cell fate in daughter cells, followed by embryo lethality [Beatty et al., Development, 2010; Beatty et al., Development, 2013; Rodriguez et al., Dev. Cell, 2017; Jankele et al., eLife, 2021]. Now we explain why we are drawing connections with lethality experimental data in Section 2.5.

> *(16) Improved Abstract: "...However, polarity can be restored through a combination of two modifications that have opposing effects..." This sentence could be revised for better clarity. For example, the authors could consider rephrasing it as follows: "...However, polarity restoration can be achieved by combining two modifications with opposing effects...".*

We sincerely thank the editor(s) and referee(s) for helpful advice!

Now we revise the abstract as follows:

“Abstract – However, polarity restoration can be achieved by combining two modifications with opposing effects.”

> *(17) Conservation of Mass in Network Models: Is conservation of mass satisfied in their network models?*

We sincerely thank the editor (s) and referee(s) for the comment!

While previous experiments provide evidence for near-constant protein mass during the establishment phase [Goehring et al., Science, 2011], whether this is consistent until the end of maintenance is unclear.

Many previous *C. elegans* cell polarization models have assumed mass conservation on the cell membrane and in the cell cytosol, this model description can lead to reverse spatial

concentration distribution between the cell membrane and cytosol [Fig. 3 of Seirin-Lee et al., J. Theor. Biol., 2016; Fig. 2ab of Seirin-Lee et al., J. Math. Biol., 2020], disobeying experimental observation [Fig. 4A of Sailer et al., Dev. Cell, 2015; Fig. 1A of Lim et al., Cell Rep., 2021]. This implies that mass conservation may be inappropriate in modeling the real spatial concentration distributions distinguished between the cell membrane and cytosol. To address this issue, some theoretical research incorporated protein production and degradation into their model, instead of assuming mass conservation [Tostevin et al., Biophys. J., 2008]. More definitive experimental data on the spatiotemporal changes in protein mass are essential for constructing a more accurate model.

Given the absence of a universally accepted model in agreement with experimental observation, we adopted the assumption that the concentration of molecules in the cytosol (not the total mass on the cell membrane and in the cell cytosol) is spatially inhomogeneous and temporally constant, which was also used before [Kravtsova et al., Bull. Math. Biol., 2014]. In the context of this well-mixed constant cytoplasmic concentration, our model successfully reproduced the cell polarization phenotype in wild-type and eight perturbed conditions (Section 2.5; Fig. S7; Fig. S8), supporting the validity of this simplified, yet effective, model. Now we have provided a discussion of protein mass assumption to foster a more comprehensive understanding in the future.

> *(18) Comparison of Network Structures: In Figure 1c, the authors demonstrate that the symmetric two-node network is susceptible to single-sided additional regulation. They considered four subtypes of modifications, depending on whether [L] is in the anterior or posterior and whether [A] and [L] are mutually activating or inhibiting. What is the difference between the structure where [L] is in the anterior and in the posterior? Upon comparing the time evolution of the left panel ([L] is sided with*
>
> *) and the right panel ([L] is sided with [A]), the difference is so tiny that they are almost indistinguishable. It might be beneficial for the authors to provide a clearer explanation of the differences between these network structures to aid in understanding their implications.*

We sincerely thank the editor(s) and referee(s) for the constructive suggestion!

The difference between the structures where [L] is in the anterior and posterior is the initial spatial concentration distribution of [L], which is polarized to have a higher concentration in the anterior and posterior respectively. The time evolution of the left panel ([L] is sided with [P]) and the right panel [L] is sided with [P]) is almost indistinguishable because the perturbation from [L] is slight (less than over one order of magnitude) compared to the

predominant [A]~[P] interaction ($k_{A2}^{P} = k_{P2}^{A} = 1$ for [A]~[P] mutual inhibition while

$k_{A2}^{L} = k_{L2}^{A} = 0.025$ for [A]~[L] mutual inhibition and q_{L2}^{A} & $q_{A2}^{L} = 0.012$ for [A]~[L] mutual

activation), highlighting the response of cell polarization pattern. To aid the readers in understanding their implications, we have added the [L] and plotted the spatial concentration distribution of all three molecular species at t=0,100, 200, 300, 400 and 500 in Fig. S3, where the difference between the [L] ones in the left and right panels are distinguishably shown.

> *(19) Figure Reference: In line 308, Fig. 4a is referenced when explaining the loss of pattern stability by modifying an individual parameter, but this is not shown in that panel. Please update the panel or adjust the reference in the main text.*

We sincerely thank the editor(s) and referee(s) for pointing out this problem!

Fig. 4 focuses on the regulatable shift of the zero-velocity interface by modifying a pair of individual parameters, not on the loss (or recovery) of pattern stability, which has been analyzed as a focus in Fig. 1, Fig. 2, and Fig. 3. Fig. 4a is actually from the same simulation as the one in Fig. 1a, which has spatially uniform parameters used as a reference in Fig. 4. The individual parameter modification in other subfigures of Fig. 4 shows how the zero-velocity interface is shifted in a regulatable manner always in the context of pattern stability. Now we update the panel, adjust the reference, add one more paragraph, and improve the wording to clarify how the analyses in Fig. 4 are carried out on top of the pattern stability already studied.

> *(20) Viable Parameter Sets: In line 355, the number of viable parameter sets (602) is not very informative by itself. We suggest reporting the fraction or percentage of sets tested that resulted in viable results instead. This applies similarly to lines 411 and 468.*

We sincerely thank the editor(s) and referee(s) for the constructive comment!

Now the fraction/percentage of parameter sets tested that resulted in viable results are added everywhere the number appears.

> *(21) Perturbation Experiments: In lines 358-359, "the perturbation experiments" implies that those considered are the only possible ones. Please rephrase to clarify.*

We sincerely thank the editor(s) and referee(s) for the helpful advice!

Now we rephrase three paragraphs to clarify why the perturbation experiments involved with [L] and [C] are considered instead of other possible ones.

> *(22) Figure 2S: This figure is unclear. The caption states that panel (a) shows the "final concentration distribution," but only a line is shown. If "distribution" refers to spatial distribution, please clarify which parameters are shown.*

We sincerely thank the editor(s) and referee(s) for pointing out this problem!

Now we clarify the “spatial concentration distribution” and which parameters are shown in the figure caption.

> *(23) Figure 5 and 6 Captions: The captions for Figures 5 and 6 could benefit from clarification for better understanding.*

We sincerely thank the editor(s) and referee(s) for the constructive suggestion!

Now we clarify the details in the captions of Fig. 5 and Fig. 6 for better understanding.

> *(24) Figure 5 Legend: The legend on the bottom right corner of Figure 5 is unclear. Please specify to which panel it refers.*

We sincerely thank the editor(s) and referee(s) for the constructive suggestion!

Now we clarify to which the legend on the bottom right corner of Fig. 5 refers.

> *(25) L and A~C Interactions: In paragraphs 405-418, please explain why the L and A~C interactions are removed for the comparison instead of others.*

We sincerely thank the editor(s) and referee(s) for the constructive suggestion!

Now we add a separate paragraph and a supplemental figure to explain why the L and A~C interactions are removed for the comparison instead of others.

> *(26) Network Structures in Figure S3: From the "34 possible network structures" considered in Figure S3 (lines 440-441), why are the "null cases" (L disconnected from the network) relevant? Shouldn't only 32 networks be considered?*

We sincerely thank the editor(s) and referee(s) for pointing out this problem!

Now the two “null cases” are removed:

> *(27) Figure S3 Caption: The caption must state that the position of the nodes (left or right) implies the polarisation pattern. Additionally, with the current size of the figure, the dashed lines are extremely hard to differentiate from the continuous lines.*

We sincerely thank the editor(s) and referee(s) for the constructive suggestion!

Now we state that the position of the nodes (left or right) implies the polarization pattern. Additionally, we have modified the figure size and dashed lines so that the dash lines are adequately distinguishable from the continuous lines.

> *(28) Equation #7: It is confusing to use P as the number of independent simulations when P is also one of the variables/species in the network. Please consider using different notation.*

We sincerely thank the editor(s) and refer(s) for the hhelpful advice!

Now we replace the P in current Equation #8 with Q and the P in current Equation #10 with W.

> *(29) Use of "Detailed Balance": The authors used the term "detailed balance" to describe the intricate balance between the two groups of proteins when forming a polarised pattern. However, "detailed balance" is a term with a specific meaning in thermodynamics. Breaking detailed balance is a feature of nonequilibrium systems, and the polarisation phenomenon is evidently a nonequilibrium process. Using the term "detailed balance" may cause confusion, especially for readers with a physics background. It might be advisable to reconsider the terminology to avoid potential confusion and ensure clarity for readers.*

We sincerely thank the editor(s) and referee(s) for the constructive suggestion!

To avoid potential confusion and ensure clarity for readers, now we replace “detailed balance” with “balance”, “required balance”, or “interplay” regarding different contexts.

> *(30) Terminology: The word "molecule" is used where "molecular species" would be more appropriate, e.g., lines 456 and 551. Please revise these instances.*

We sincerely thank the editor(s) and referee(s) for the constructive suggestion!

Now we replace all the “molecule” by “molecular species” as suggested.

> *(31) Section 2.5: This section is confusing. It isn't clear where the "method outlined" (line 464) is nor what "span an iso-velocity surface at vanishing speed" means in line 470. The sentence in lines 486-488, "An expression similar to Eq. 8 enables quantitative*

> *prediction...", is too vague. Please clarify these points and specify what the "similar expression" is and where it can be found.*

We sincerely thank the editor(s) and referee(s) for the constructive suggestion!

Now we clarify these points and specify the terms as suggested.

> *(32) Software Mention: The software is only mentioned in the abstract and conclusions. It should also be mentioned where the computational pipeline is described, and the instructions available in the supplementary information need to be referenced in the main text.*

We sincerely thank the editor(s) and referee(s) for pointing out this problem!

Now we mention the software where the computational pipeline is described and reference the instructions available in the Supplemental Text.

> *(33) Supplementary Material References: Several parts of the supplementary material are never referenced in the main text, including Figure S1, Movies S3-S4, and the Instructions for PolarSim. Please reference these in the main text to clarify their relevance and how they fit with the manuscript's narrative.*

We sincerely thank the editor(s) and referee(s) for pointing out this problem!

Now we add all the missing references for supplementary materials to the main text properly.

https://doi.org/10.7554/eLife.96421.2.sa0